



Novel 1,2,3-triazole-tethered Pam₃CAG conjugates as potential TLR-2 agonistic vaccine adjuvants

Tukaram B. Mhamane^{a,b,1}, Shainy Sambyal^{a,b,1}, Sravanthi Vemireddy^{a,b}, Imran A. Khan^c, Syed Shafi^c, Sampath Kumar Halmuthur M.^{a,b,*}

^a Vaccine Immunology Laboratory, OSPC Division, CSIR-Indian Institute of Chemical Technology, Hyderabad 500007, India

^b Academy of Scientific and Innovative Research (AcSIR), Ghaziabad, Uttar Pradesh 201 002, India

^c Department of Chemistry, School of Chemical and Life Sciences, Jamia Hamdard, New Delhi

ARTICLE INFO

Keywords:

TLR-2
Pam₃CAG-triazole conjugate
Click chemistry
Adjuvant
HBsAg
IgG
CD4
CD8

ABSTRACT

A focused library of water soluble 1,2,3-triazole tethered glycopeptide conjugates derived from variety of azido-monosaccharides and aliphatic azido-alcohols were synthesized through manipulation at the C-terminus of Pam₃CAG and screened for their potential as TLR2 agonistic adjuvants against HBsAg antigen. In vitro ligand induced TLR2 signal activation was observed with all the analogues upon treatment with HEK blue TLR2 cell lines. Conjugate derived from ribose (6e), which exhibited pronounced HBsAg specific antibody (IgG) titer also shown enhanced CD8⁺ population indicating superior cell mediated immunity compared to standard adjuvant Pam₃CSK₄. Further, docking studies revealed ligand induced heterodimerization between TLR1 and 2. Overall, the result indicates the usefulness of novel conjugates as potential vaccine adjuvant.

1. Introduction

Importance of new immune adjuvants is steadily increasing with the growing demand for safe and highly efficacious vaccines against old as well as emerging viral diseases. With the availability of repository of subunit antigens for various diseases, there has been a need for developing novel PRR agonists with varying degrees of Th1/Th2 activation, required for eliciting qualitatively specific immune response with particular antigens [1–3]. Activation of innate and adaptive immune response through heterodimerization of TLRs induced by these PRR agonists is well established. Inspired by the structure of bacterial lipoprotein derived N-terminal amino acid S-(2,3 dihydroxypropyl)-L-cysteine lipid head group, libraries of novel triacylated and diacylated cysteinyl lipopeptides have been developed, which act through TLR1/2 and TLR2/6 heterodimerization respectively [4,5]. Evolutionarily, such TLR heterodimerization enable recognition of continuous ligand field expansion of pathogen associated molecular patterns encompassing structural changes in lipid head group. Such glycolipid adjuvants can be administered either in combination with an antigen or can be covalently conjugated to an antigenic peptide to elicit desired immune response. Even though the molecular mechanism for ligand recognition by TLRs is

not fully understood so far, amphiphilicity of these cysteinyl glycolipids has been recognized as key feature that influence their TLR activation propensity. The important role played by TLR2 in regulating the host immune response to pathogens, led researchers to develop several new structural analogues of natural N-apalmitoyl-S-[2,3-bis(palmitoyloxy)-(2R)-propyl]-L-cysteinyl peptides tuning its amphiphilicity to suit their application in different vaccine developments. In this context, the N-terminal part of the 44-kDa lipoprotein LP44 of *Mycoplasma salivarium* or Braun lipoprotein, have all been described as TLR2 agonists, their simpler synthetic analogues S-[2,3-bis(palmitoyloxy)-(2R)-propyl]-R-cysteinyl lipopeptides, like 'Pam₂CAG' and Pam₃CysSK₄, have also shown TLR2 agonist activity and can therefore be considered as more useful and easily attainable immunoadjuvants. However, non-specific adhering of highly amphiphilic polycationic lysine peptide entities make this more unsuitable for vaccine application as they complicate the preparation of the vaccine formulation cocktail. Amphiphilic lipopeptides, such as Pam₃CAG (N-palmitoyl-S-[2,3-bis(palmitoyloxy)-(2R)-propyl]-L-cysteinyl-L-alanyl-glycine) synthesized by Benoit et al. effectively induced the proliferation of BALB/c mouse splenocyte *in vitro* when incorporated into liposomes [6]. The lipid head group of this synthetic lipopeptide interacted with lipid bilayer of liposome whereas

* Corresponding author at: Vaccine Immunology Laboratory, OSPC Division, CSIR-Indian Institute of Chemical Technology, Hyderabad 500007, India.

E-mail address: sampath.iict@gov.in (S.K. Halmuthur M.).

¹ Equal authorship.

their hydrophilic tail was covalently modified to anchor one or two peptide containing T epitopes against which an immune response was elicited [7,8]. On the contrary, whenever liposomal formulation is not desirable, the amphiphilicity of these lipopeptide becomes a serious drawback, hampering ease of its usage as immune adjuvants both *in vitro* and *in vivo* [9]. Several studies revealed the loss of activity owing to large heterogeneous aggregates of such amphiphilic lipopeptides in solutions, rendering its activity critically dependent on the presence of proteins like bovine serum albumin or solubiliser detergents such as octyl- β -D-glucopyranoside, and even on the protocol of dilution (e.g., with *tert*-butyl alcohol or dimethyl sulfoxide) [10]. As a possible solution to these difficulties, Benoit et al. further developed hydrophilic PEG conjugates of Pam₃CAG and demonstrated their ability to induce mouse dendritic cell maturation and B cell proliferation *in vitro* [6,11]. In spite of these efforts, their actual usefulness as vaccine adjuvants *in vivo* - a true testimony for their adjuvanticity, has not been demonstrated.

In continued efforts of Halmuthur MSK et al. to develop novel vaccine adjuvants and delivery systems, first successful attempt of the amalgamation of carbohydrate-Pam₃Cys motifs tethered to a 1,2,3-triazole linker as a peptide free TLR2 adjuvants [12]. The 1,2,3-triazole based derivatives have been employed in various medicinal chemistry applications, such as anti HIV [13], antiviral, anticancer [14], anticonvulsant [15], antiallergic [16] and antifungal [17] agents. α -GalCer is the most potent agonistic antigen of a natural killer T-cell receptor. Lee et al. prepared a series of 1,2,3-triazole-containing α -GalCer analogues in which the lipid chain lengths were incrementally varied. Isosteric replacement of the amide moiety of α -GalCer with a triazole increased the IL-4 versus IFN- γ bias of released cytokines [18]. The isosteric replacement of amide with 1,2,3-triazole scaffold in α -GalCer stimulated higher levels of both IFN- γ and IL-4 cytokine expression *in vitro* compared to that of α -GalCer [19]. Mohamed R. Aouad et al. have reported different 1,2,3-triazole conjugates with anti microbial [20–24], anticancer [25–29] and antitubercular [30] properties. Some of the 1,2,3-triazole containing drugs and other bioactive compounds have been depicted in Fig. 1.

1,3-Dipolar Huisgen cycloaddition of organic azides with alkynes has been recognized as the most widely reported method for the construction of 1,2,3-triazole scaffold. Herein, we present the synthesis and *in vivo* adjuvanticity of some novel 1,2,3-triazole tethered Pam₃CAG-

carbohydrate/aliphatic alcohol conjugates against HBsAg antigen. When tested in murine model, these ligands show TLR2 agonistic propensity and DC activation *in vitro*. Furthermore, ligand induced heterodimerization between TLR1 and TLR2 has been demonstrated by *in silico* docking studies.

2. Materials and methods

2.1. Chemistry

All reagents which are commercially available were used without further purification and purchased from Sigma Aldrich, if not indicated otherwise. All organic solvents were dried and freshly distilled before use wherever necessary by using standard procedures. Tetrahydrofuran (THF) was dried and distilled from freshly extruded Na wires and Dichloromethane (DCM) purified by overnight stirring with CaH₂ followed by distillation. All the moisture sensitive reactions were performed in the oven dried glass wares under inert atmosphere of nitrogen or argon. All the chemical transformations were monitored by using Thin Layer Chromatography (TLC) on a 2–5 cm percolated E. Merck Silica Gel 60 F254 plates (0.25 mm) and spots were visualized using UV lamp. Staining was developed with Iodine or by dipping TLC in p-Anisaldehyde or 10% Phosphomolybdic acid solution in EtOH and then charred on a hot plate. Removal of solvent or concentration under reduced pressure was performed using a rotary evaporator at 25–40 °C. Column chromatography was carried out by using silica gel (Merck 60-120mesh) and (Merck 100–200 mesh) with technical grade ethyl acetate/hexane and chloroform/methanol as eluents. All melting points were determined on a Buchi capillary melting point apparatus and are uncorrected. NMR spectra were recorded with a Bruker AC-300 MHz, a Bruker AM-400 MHz and a Bruker AMX-500 MHz spectrometer instruments in CDCl₃, CD₃OD and DMSO-*d*₆ with (CH₃)₄Si as an internal standard for ¹H NMR spectra and solvent signals as internal standard for ¹³C NMR spectra at ambient temperature. Chemical shifts (δ) are reported in ppm. Coupling constants J were reported in Hz. NMR signal splitting patterns were designated as follows: s - singlet, d - doublet, dd - doublet of doublet, dt - doublet of triplet, td - triplet of doublet, t - triplet, q - quartet, p - pentet, bs - broad singlet, m - multiplet, br - broad. For ESI-MS, *m/z* values are reported in atomic mass units and recorded in Shimadzu

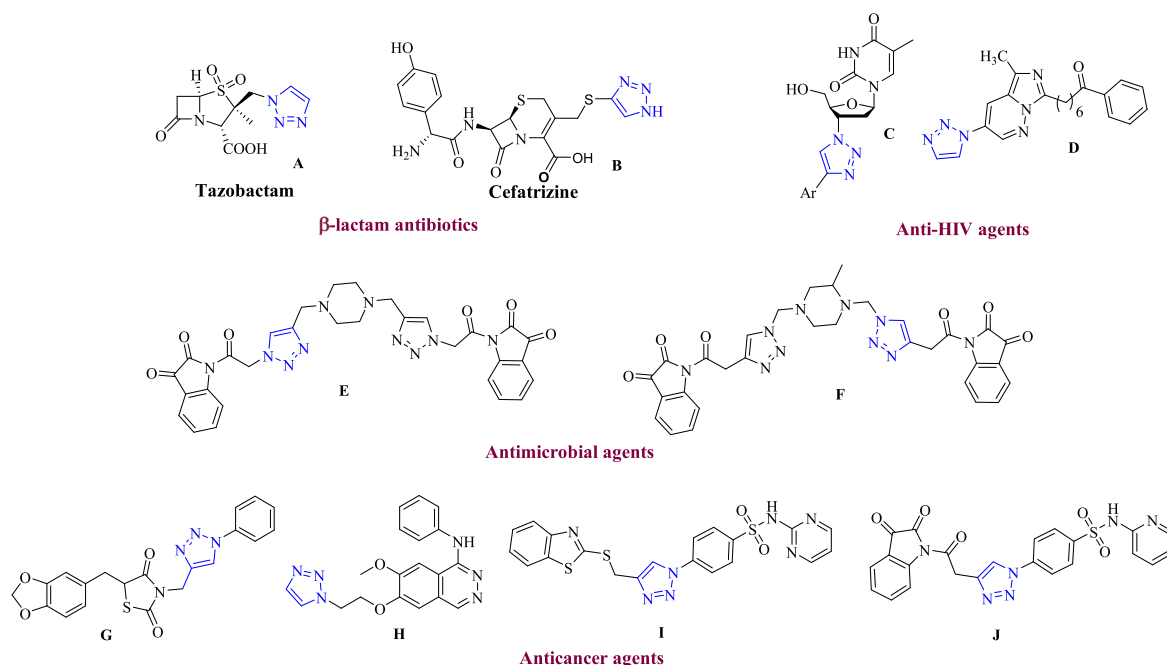


Fig. 1. Some examples of 1,2,3-triazole containing drugs and bioactive molecules.

instrument.

2.1.1. Synthesis of new 1,2,3-triazolyl tethered Pam3CAG conjugates

Seven new Pam₃CAG conjugates have been designed, comprising different carbohydrates and simple aliphatic alcohols, tethered together through a 1,2,3-triazol-4-yl methanamine spacer employing azide-alkyne click chemistry approach (Fig. 2). Carbohydrate employed include both furanosyl and pyranosyl entities lined to peptide at anomeric or primary hydroxyl position.

Synthesis of target conjugates **6a-g** includes the preparation of three key fragments viz., Pam₃Cys-OH (**2**) the lipid head group mainly responsible for TLR agonistic activity, Boc-Ala-Gly-propargyl **4** (dipeptide alkyne) and different hydrophilic azides (I-VII).

A lipopeptide backbone skeleton Pam₃Cys-OH mainly responsible for the agonistic activity was synthesized in twelve steps [32]. Lipid head group was synthesized starting from cyclohexylidene protected vicinal diol of D-mannitol which was further subjected to oxidative cleavage to give (R)-2,3-O-Cyclohexylidene-D-glyceraldehyde. The aldehyde formed in the previous step was reduced to (R)-1,4-dioxaspiro[4.5]decan-2-ylmethanol **1** by using NaBH₄/methanol (Scheme1) [31]. Conversion of aldehyde to corresponding alcohol **1** was confirmed by the appearance of a new double doublet at δ 3.73 & 3.57 ppm corresponds to two protons in ¹H NMR spectra and a mass peak observed at m/z 195.10 [M + Na⁺] in ESI-MS. This hydroxyl compound was further treated with iodine, triphenylphosphine and imidazole to afford the corresponding iodo compound. This iodo compound later on reacted with commercial N-Boc-L-Cys-methyl ester in presence of DIPEA in DMF to afford orthogonally protected cysteine coupled protected glycerol moiety which is confirmed by ¹H, ¹³C NMR and ESI. S-alkylation of cysteine was confirmed by the appearance of the peaks corresponding to both cysteine (chemical shifts at δ 3.76 (s,3H), 1.45 (s, 9H) corresponds to methyl ester and -NH₂Boc groups respectively in ¹H NMR spectra and protected glycerol moieties and an up field shift of methylene (-CH₂-) proton signal of glycerol moiety. A mass peak at 412.30 [M + Na⁺] in ESI-MS has finally confirmed the S-alkylation of cysteine. Cysteiny methyl ester was then hydrolyzed with LiOH in THF/water (1:1) to afford corresponding carboxylic acid which was directly subjected to phenacylation with phenacyl bromide/KF to yield phenacyl ester. Appearance of the peaks at aromatic region (δ 7.89–7.49(5H).) and the disappearance of the peak corresponds to methyl ester in ¹H NMR confirms the phenacyl protection of the carboxylic acid. This structure assignment was supported by ¹³C NMR spectra in which observed signals at δ 191.78 for carbonyl of phenacyl, 170.67 carbonyl of ester, 155.50 (-C=O of Boc), 134.29–127.80 for aromatic carbons. ESI-MS

peak at m/z 516 [M + Na⁺] further confirms the product formation.

This phenacyl ester was further subjected to cyclohexylidene deprotection by using 70% AcOH gave diol **S4** which was confirmed by absence of peaks related to cyclohexane in its ¹H NMR and ¹³C NMR spectra. This structure assignment was further confirmed with its observed ESI-MS peak at m/z 436.452 [M + Na⁺]. This diol compound **S4** was subjected to dipalmitoylation by using palmitic acid under DIC/DMAP condition to furnish protected Pam₂Cys dilipidated compound which is confirmed by its ESI-MS peak at m/z 912.45 [M + Na⁺] and the proton signals corresponds to palmitoyl group in ¹H NMR. To obtain trilipidated acid compound **2**, corresponding di-palmitoylated precursor was subjected to N-Boc deprotection using 20% TFA/DCM followed by coupling of free amine with palmitic acid under EDC.HCl/HOBt condition to yield protected tri-palmitoylated compound **S5** which was supported by its ¹H NMR signals at δ 7.90–7.60(5H) for aromatic protons, δ 2.30–1.25 ppm for -CH₂- of three ester chains and δ 0.87 (t, J = 6.4 Hz, 9H.) for terminal -CH₃ of lipid chains. Further assigned structure of **S5** was confirmed by the presence of five signals ranging between δ 191.27–170.49 ppm corresponds to carbonyl carbons in ¹³C NMR (signal at δ 191.27 corresponds to benzoyl carbon of the phenacyl group, signals at δ 173.40 and 173.31 corresponds to carbonyl carbons of two palmitoyl esters, signal at δ 173.16 carbonyl of phenacyl ester and a signal at δ 170.49 corresponds amide carbonyl) and δ 134.15–127.78 for aromatic carbons. Formation of the compound **S5** is further evidenced by its observed mass at 1050.7797 [M + Na]⁺. Phenacyl protected tri-palmitoylated compound (**S5**) thus obtained was treated with activated Zn/AcOH to afford Pam₃Cys-OH (**2**) [32] (Scheme 1) in good yield which was confirmed by the absence of aromatic region in the ¹H and ¹³C spectra, further evidenced by its ESI-MS peak at m/z 932.50 [M + Na]⁺.

Synthetic pathway for another fragment Boc-Ala-Gly-Propargyl dipeptide **4** is presented in scheme 2. Mixed anhydride coupling of Boc-alanine and ethyl glycinate afforded ethyl ester of dipeptide **3** which is confirmed by its observed mass at m/z 297.25 [M + Na⁺] in ESI-MS. Further supported by the signals of ethyl at δ 4.08 (q, J = 7.1 Hz, 2H) for two protons, 1.37 (s, 9H) for Boc methyl, 1.21–1.15 for three protons from ethyl group & β -CH₃ of alanine. This was further evidenced by its ¹³C signals at δ 173.16 for carbonyl of alanine, 169.60 for -C=O glycine and 154.87 for carbonyl of Boc group. Compound **3** was subjected to hydrolysis gave Boc-Ala-Gly-OH in good yield [33]. This was used without further purification for the amide coupling with propargyl amine to obtain required building block propargylated Boc-Ala-Gly-(**4**) (Scheme 2). Compound **4** was confirmed by HRMS-MS peak at m/z 306.25 [M + Na]⁺. Further evidenced with observed peaks at δ 2.20 (t, J

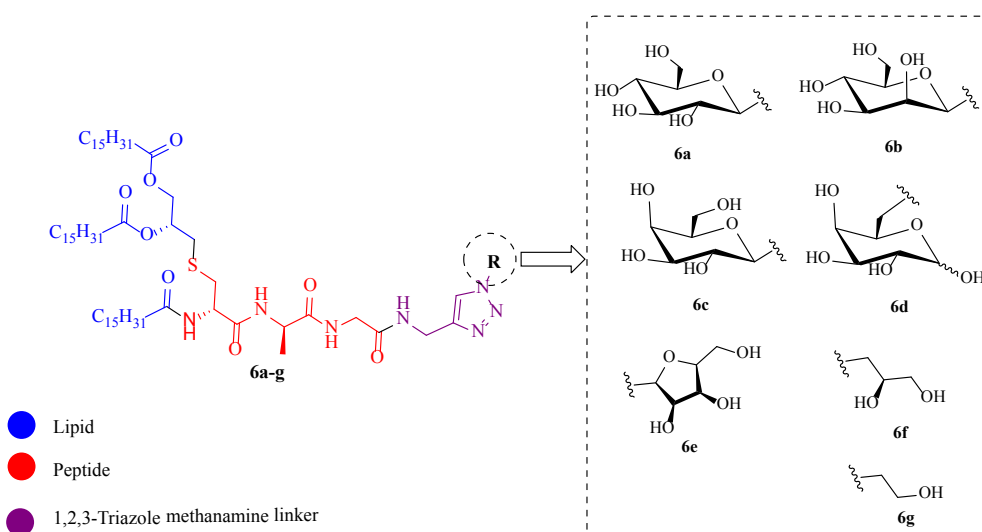
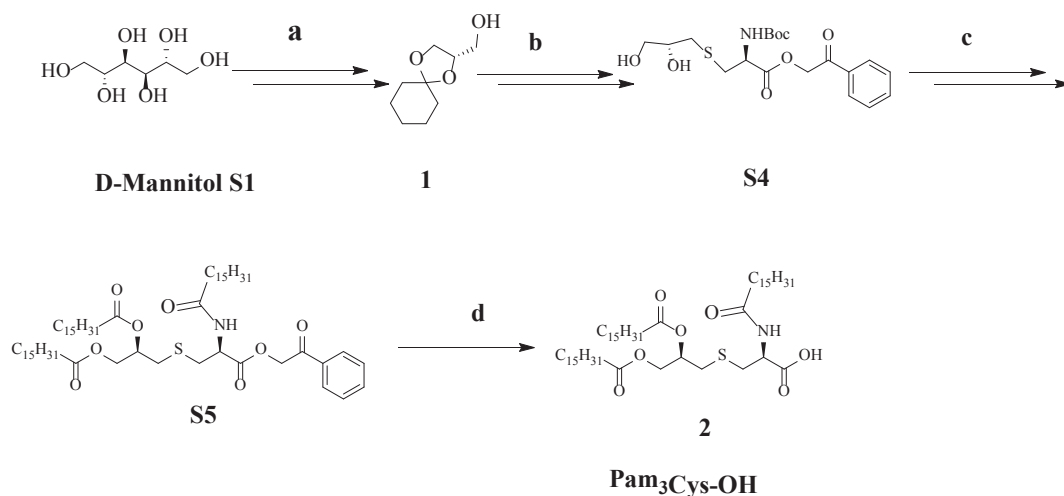
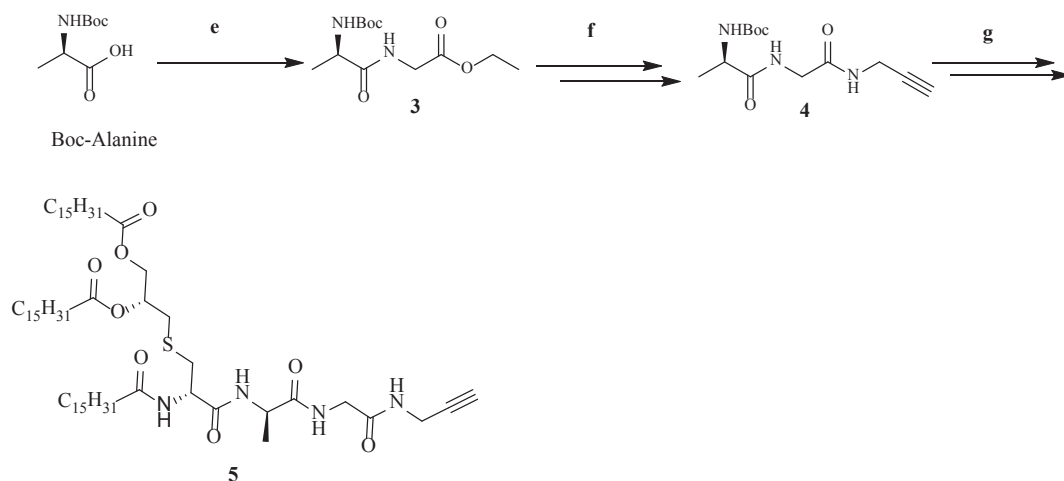


Fig. 2. Design of target molecules.

Scheme 1. Synthesis of Pam₃Cys-OH.Scheme 2. Synthesis of terminal alkyne-Pam₃CAG conjugate.

= 2.5 Hz, 1H) for propargyl proton in ¹H NMR and signals at δ 78.68, 70.78 for both alkyne carbons in ¹³C spectra. This dipeptide on further treatment with 20% TFA/DCM and coupling with previously synthesized lipid head group Pam₃Cys-OH (2) afforded Pam₃Cys-Ala-Gly-Propargyl lipopeptide (Pam₃-CAG-propargyl) 5 (Scheme 2) in moderate yields. Pam₃CAG-propargyl compound 5 was confirmed by the characteristic signals of long chains and propargyl moiety. Presence of signals at δ 0.82(t, *J* = 6.4 Hz, 9H) for terminal methyl groups, methylene protons in the range of δ (2.33–1.20) and signal for β-methyl of alanine at δ 1.35 (d, *J* = 7.2 Hz, 3H) confirmed the formation of 5. It is further supported by the observed signals in ¹³C spectra at δ 79.04, 70.06 for alkyne carbons, δ 33.98–21.17 for carbons of methylene of long chains, and δ 16.58 for β-CH₃ alanine & δ 13.71 for terminal methyl of long chains. Observed ESI-MS peak at 1097.8274 [M + Na]⁺ further evidenced the structure.

Required sugar azides were synthesized from corresponding per acetylated sugars which was subjected to azidation by using TMS-N₃/SnCl₄ gives per acetylated anomeric (α/β) azides which further treated with NaOMe/MeOH gives free hydroxyl azides (I–V) in quantitative yields [34–37]. 3-azidopropane-1, 2-diol (VI) was prepared from glycerol in good yield [38]. 2-azidoethanol (VII) was synthesized from commercially available 2-bromoethanol and NaN₃ at 80 °C in 90% yield [39].

2.2. Biology

2.2.1. Ligand induced TLR2 activation by SEAP assay

The assay was performed as per the manufacturer's instructions. HEK-Blue™ hTLR2 cells (280,000 cells per ml) were harvested in HEK-Blue™ selection medium containing normocin treated with the compounds i.e., Pam₃CysSK₄, 6a, 6b, 6c, 6d, 6e, 6f and 6g (10 μg/ml) and the plates were incubated at 37 °C in 5% CO₂ for 24 h. Stimulation with a TLR2 ligand activates NF-κB which induce the production of SEAP (secreted embryonic alkaline phosphatase). The levels of SEAP can be observed with naked eye and determined using a spectrometer at 620–655 nm.

2.2.2. Ex vivo activity

2.2.2.1. Immunization. Female BALB/c mice (8–9 weeks) were purchased from CSIR-CCMB, Hyderabad, All animal experiments were approved by the local ethical committee and animals were kept in accordance with CPCSEA guidelines. They were immunized with albumin, from chicken egg (Sigma-Aldrich, St. Louis, MO) 100 μg in 100 μl at 0th day and sacrificed on 7th day and the spleen were collected.

2.2.2.2. Cell preparation. Mice were sacrificed 7 days post injection; spleens were harvested in PBS and processed on ice to single-cell

suspensions by frosted slides. The cell suspension was further passed through cell strainer to remove the debris. Then they were centrifuged at 2000 rpm for 10 min and ACK lysis buffer was then added to lyse the erythrocytes. PBS saline wash was given thrice to the cell pellet. Cells were re-suspended in complete RPMI 1640 medium with 10% FBS. Viable cell concentration was determined by trypan blue staining.

2.2.2.3. Re-stimulation of splenocytes. 1×10^5 Splenocytes/well in 96-well plates were cultured in complete RPMI medium with 10% FBS and re-stimulated with 20 $\mu\text{g}/\text{mL}$ of ovalbumin (Sigma-Aldrich, St. Louis, MO). Cells were treated with 6 different (M1-6) compounds at a concentration of 1, 10 and 100 $\mu\text{g}/\text{ml}$. Pam₃CysSK₄ (Vacci Grade™ InvivoGen, USA) was used as a control. Treated cells were incubated for 48 h at 37 °C in 5% CO₂ incubator. Supernatants were harvested and checked for cytokine expression. They were stored at 70 °C until further analysis.

2.2.2.4. Cytokine estimation – sandwich ELISA. Quantification of pro inflammatory cytokines IL-6 and TNF-alpha from cell supernatant of splenocytes treated with compounds at three different concentrations was carried out by Opti Elisa Kit (BD) according to manufacturer's protocol. Briefly 1×10^5 cells/well were seeded in 12 well plates and incubated at 37 °C with 5% CO₂ for 48 h. The supernatant was collected from each well separately for cytokine estimation by coating ELISA plates with purified anti-mouse antibody IL-6 and TNF- α diluted with bicarbonate-carbonate buffer and incubated at 4 °C overnight. Plates were washed thrice with PBST 20 and blocked with 100 μl of 1% BSA. After 1 h incubation at RT, plates were again washed thrice with same washing buffer. 100 μl of serum sample was added along with serially diluted recombinant antibody (IL-6 and TNF- α). Plates were incubated for 3 h at 37 °C. Post incubation was followed by four times washing and then addition of detection antibody prepared in BSA with 1 h incubation at RT. After four times washing, HRP streptavidin (1:3000) in 1% BSA was added 100 μl each and kept for incubation for 30 min at RT. TMB substrate was added after thrice washing and kept for incubation till development of color or for 15 min. The reaction was stopped by adding 50 μl of 2 N H₂SO₄ and the absorbance was measured at 450 nm in ELISA reader (Tecan, Infinite pro).

2.2.3. In vivo activity studies

2.2.3.1. Immunization methods. For detail study Balb/c female mice were used, purchased from Palamur Biosciences Private Limited, Hyderabad. All the experiments on animals were approved by the Institutional Animal Ethics Committee (IAEC) of CSIRIICT for 168 nos of Balb/c mice with IAEC approval number: IICT/IAEC/014/2019. 71 Balb/c female mice were immunized with Pam₃Cys analogs i.e. **6a**, **6b**, **6c**, **6d**, **6e**, **6f** and **6g** each 1 mg/10 μl . Along with this Pam₃CysSK₄ standard (20 $\mu\text{g}/\text{dose}$) and HbsAg (1 $\mu\text{g}/\text{dose}$) was also used for immunization i.e. 1 mg/ml each. Immunization was done to different groups with varying concentration i.e. 10, 20, 30 $\mu\text{g}/\text{dose}$. The mice were provided with booster dose on 14th day and were sacrificed on 28th day of immunization.

2.2.3.2. Serum collection. To measure the count of antibody against that particular antigen, retro-orbital blood was collected separately from each group on 28th day. The blood was centrifuged at 2000 rpm for 20 min at RT. Serum was carefully collected in eppendorf tubes and stored at 40 °C for estimation of IgG titer.

2.2.3.3. IgG titer – indirect ELISA. ELISA plates (HIMEDIA, Mumbai) were coated with HbsAg (1 $\mu\text{g}/\text{ml}$) diluted in bicarbonate-carbonate buffer having pH 9.4 and incubated overnight at 4 °C. Thrice plates were washed with PBS Tween20 (pH 7.4) and blocked with 1% BSA (100 $\mu\text{l}/\text{well}$) to prohibit non-specific binding with 1 h incubation at RT.

Again plates were washed 3 times with PBS Tween20 followed by the addition of serially diluted serum sample in 1% BSA with 2 h incubation at 37 °C. After 4 times washing, HRP goat anti-mouse IgG (1:3000) in 1% BSA was added to plates and kept for 1 h incubation at RT. Plates were washed with PBS Tween20 3 times. 100 μl of TMB substrate (TMB reagent A + B in equal volume) was added to each well and incubates in dark at RT for about 15 min or till color development. The reaction was stopped by adding stopping reagent i.e. 2 N H₂SO₄, 50 $\mu\text{l}/\text{well}$ and absorbance was measured at 450 nm by using multimode reader (Tecan, Infinite pro).

2.2.3.4. Spleen collection and splenocyte isolation. Spleen was collected only from those groups which showed good IgG titer for further studies. Mice were sacrificed and spleen was collected in chilled PBS. The flesh was cleaned in PBS and spleen was homogenized in RPMI media (900 ml autoclaved water, 1 packet of RPMI 1640 (HIMEDIA, Mumbai), 2.0 g sodium bicarbonate, 10 ml antibiotic antimycotic solution 100x, 10 ml penicillin streptomycin 2x, 3.94 μl 2-mercaptoethanol, 100 ml FBS) on 0.22 μm filter by applying pressure with syringe. The filtrate was collected in 50 ml Tarson tube and centrifuged for 10 min at 2000 rpm at 4 °C. ACK (1 ml/spleen) treatment was given to the pellets for 1 min 30 s. PBS wash and then cell count.

2.2.3.5. Immunophenotyping. Splenocytes prepared in RPMI media from immunized mice were taken for immunophenotyping. 3×10^5 cells from each group were taken separately to FACS tubes and washed with staining buffer. Fc blocker was added 1 $\mu\text{l}/\text{tube}$ and incubated for 15 min at 4 °C. After incubation cells were washed twice with staining buffer. Fluorochrome characterized antibodies (FITC-A antiCD4 and APC-Cy7-A antiCD8) were added to each tube and incubated for 30 min at 4 °C. Again tubes were centrifuged with staining buffer. Cells were collected and resuspended in sheath fluid for analysis using BD FACS suit software.

2.2.3.6. Splenocyte proliferation. Splenocytes from each group of selected immunized mice were seeded in 96 well plates with cell count 1×10^5 cells/well. The cells were restimulated by using HBsAg, LPS and ConA with concentration 0.1, 10 and 2 $\mu\text{g}/\text{ml}$ respectively. The plates were incubated at 37 °C for 48 h having 5% CO₂. After the completion of incubation, MTT reagent (5 mg/ml PBS) was added to the cells i.e. 20 $\mu\text{l}/\text{well}$ and incubated for 3 h at 37 °C. The untransformed MTT was removed (50 μl each) and was recovered by 50 μl of DMSO, followed by 15 min incubation at RT. The absorbance was measured at 630 nm and % proliferation of the cells was calculated by keeping cell control as reference [40].

2.2.4. DC activation (CD86 and MHC II)

The EasySep™ Pan Dendritic Cell Isolation Kit, (MACS Miltenyi Biotec-Germany) mouse, is a fast enrichment kit for untouched isolation of all dendritic cell subpopulations. Isolation assay was performed as per the manufacturer's instructions. Briefly, cells were prepared (1×10^8 cells/ml) in the range of 0.25–2.0 ml and sample was added to 5.0 ml tubes. Enrichment cocktail (50 $\mu\text{l}/\text{ml}$) was added to the cells, which was mixed well and incubated at 2–8 °C for 15 min. The cells were then washed with the recommended medium and centrifuged at 300g for 10 min. Supernatant was discarded and was resuspended in the original volume of 0.25–2.0 ml with recommended medium. This was followed by adding the Biotin selection cocktail (100 $\mu\text{l}/\text{ml}$) to the cells, mixed well and was incubated at 2–8 °C for 10 min. After which, the magnetic particles were vortexed and 75 $\mu\text{l}/\text{ml}$ of it was added to the cells, which was then mixed and incubated at 2–8 °C for 10 min. Recommended medium was added to the sample, mixed gently by pipetting up and down. The tubes, without lid was inserted into the magnet and incubated at RT for 5 min. The magnet was lifted and at once inverted the magnet with tube, pouring the entire enriched cell suspension into a new

tube. The above mentioned step was repeated one more time and the isolated cells were ready for use.

Then cells were treated with standard Pam₃CysSK₄ and compounds **6e** at 20 µg concentration each for 24 h. Then cells were stained with CD86 and MHC II markers to estimate the ability of compounds to activate DCs.

2.3. Computational studies

The crystal structure of high resolution TLR1–TLR2 heterodimer with a tri-acylated lipopeptide (Pam₃CysSK₄) was downloaded from Protein Data Bank (PDB ID: 2Z7X). The resolution is 2.10 Å. The docking study with the native ligand (tri-acylated lipopeptide) and the **6a-g** molecules was performed using Schrodinger suite 2016 software. All the crystallographic water molecules and other small molecules were removed. Hydrogen atoms were added using OLPS. Then the docking protocol file was generated using the Glide-Dock module using SP and XP mode. The active site was detected using the ligand bound protein-ligand complex and was used for the detection of the gridbox with box size of 25, 30, 28. Docking was carried out in both SP and XP mode using the same gridbox. The active site was confirmed with the reference of the ligand, which was prepared using the Ligprep option. The native ligand for docking was extracted from the complex structure retrieved from Protein Data Bank. The molecular structures of **6a-g** were prepared using Chemdraw 3D software and initially all the prepared molecules were minimized using the MMFF protocol. Three conformations with the top ranking scores (top 3 conformers) for molecules **6a-g** were saved for further study. Generation of an accurate complex structure for **6a-g** of the synthesized ligands showed activity but due to large hydrophobic pockets the docking in an existing (rigid) structure of the receptor induces higher standard deviation from the experimental data. Thus, rescue of false negatives (poorly scored true binders) in virtual screening experiments, where instead of screening against a single conformation of the receptor, additional conformations obtained with the induced fit protocol are used. We performed docking of the designed ligands with TLR1, TLR2 and TLR1-TLR2. The results were concluded by opting LIAISON calculations (A Liaison simulation combines a molecular-mechanics calculation with experimental data to build a model scoring function used to correlate or to predict ligand-protein binding free energies) and MM/PBSA calculation (The binding free energy (ΔG) of the complex is calculated using molecular mechanics/Poisson–Boltzmann surface area (MM/ PBSA) approach).

3. Results

3.1. Chemistry

A focused library of seven highly regioselective 1, 4-disubstituted 1,2,3-triazole products was prepared by using click chemistry protocol (Scheme 3). Cycloaddition of compound **5** (100 mg, 0.093 mmol) and various hydrophilic azides (**I-VII**, 0.111 mmol) were carried out in the presence of CuSO₄·5H₂O (47 mg, 0.186 mmol) and sodium ascorbate

(36.82 mg, 0.186 mmol) in water:ter-butanol (5 ml, 1:1) mixture at room temperature for 8 to 12hrs which furnished the desired products **6a-g** in excellent yields. All the compounds synthesized were subjected to purification by column chromatography. The novel 1,2,3-triazole conjugates **6a-g** were fully characterized based on their ¹H and ¹³C nuclear magnetic resonance (NMR) and mass spectrometry (MS) spectra. The structures of all the compounds were in agreement with their spectroscopic data. The formation of the triazoles **6a-g** was evidenced by their ¹H NMR spectra, which revealed the absence of the terminal acetylenic proton confirming its involvement in the cycloaddition reaction.

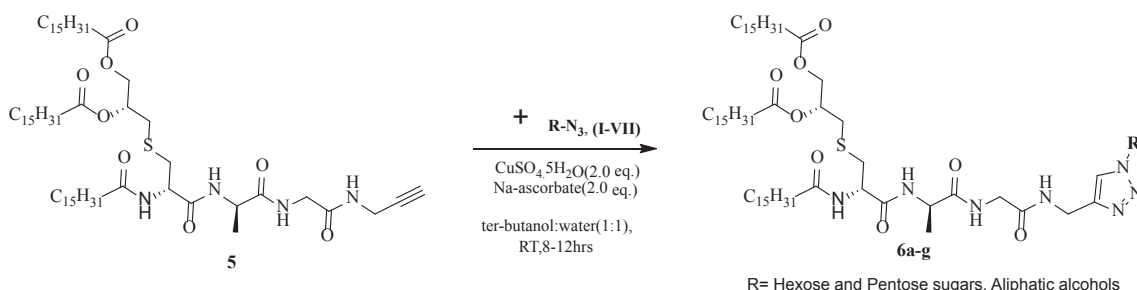
The structure of the representative compound **6a** was established on the basis of its NMR and mass spectral analysis. In the ¹H NMR spectra of **6a**, the existence of triazolyl proton at δ 7.94 ppm (s, 1H) and anomeric sugar proton of glucose at δ 5.52 ppm (d, *J* = 9.1 Hz, 1H, H-1) confirms the formation of 1,4-disubstituted 1,2,3-triazole compound. Further, the presence of signal at δ 1.39 (d, *J* = 7.1 Hz, 3H) corresponds to β-methyl of alanine and the presence of signals corresponds to long chain terminal methyl protons at 0.85 (t, *J* = 6.5 Hz, 9H) in ¹H NMR supports the product formation. All glucose protons and other deshielded protons observed in the range of δ (5.17–3.52) ppm at usual chemical shifts. This was further evidenced by its ¹³C spectra wherein all the signals observed at their usual chemical shifts i.e. δ 144.45, 121.55 characteristic peaks for triazole carbons. Ester long chains and peptidewere confirmed by carbonyl region δ 175.04 for —C=O of ester, 173.55 for —C=O of ester, 173.43 for NH—C=O of palmitoyl amide and 171.69, 171.32, 169.92 for carbonyl carbons of peptide. Observed peaks of β-methyl of alanine at δ 16.04, α-CH- of alanine, glycine, triazole-CH₂- & α-CH of cysteine at δ 52.37, 42.33, 42.20, 49.73 respectively, terminal methyl of long chains at δ 13.38 and all —CH₂- of long chains in the range of δ (33.62–22.16) further confirmed presence of peptide and long chains. D-glucose carbons were observed at δ 87.72 (C-1), 78.95 (C-5), 72.27 (C-3), 69.91 (C-4), 68.83 (C-2) and 60.62 (C-6) which further proves the conjugation of sugar with lipid head group through 1,2,3-triazole linker. The presence of signal at *m/z* 1280.9145 [M + H⁺] in ESI-HRMS finally confirms the product formation of **6a**.

A focused library of seven novel 1,2,3-triazole-tethered Pam₃CAG conjugates have been synthesized by employing the click chemistry approach and the final compounds are depicted in Table 1.

3.2. Biological activity

3.2.1. TLR specificity assay

Novel Pam₃CAG triazolyl conjugates were subjected to *in vitro* screening to evaluate the possible modulation in TLR2 specificity, potency, and binding affinity after introduction of the hydrophilic moieties derived from various monosaccharide and aliphatic alcohols. The novel analogs of Pam₃CAG were subjected to *in vitro* assay to evaluate their ligand induced TLR2 signal activation on HEK blue TLR2 cell lines and found that all analogues stimulated TLR2 in tune with the standard TLR2 ligand Pam₃CysSK₄. The results obtained were depicted in Fig. 3.



Scheme 3. Synthesis of Pam₃CAG based triazole analogues (**6a-g**).

Table 1
1,2,3-triazole-tethered Pam₃CAG conjugates.

Sr. No	Alkyne (Compound 5)	Azides R-N ₃ (I-VII)	Pam ₃ CAG conjugate (6a-g)	Yield (%)
1				93
2				91
3				88
4				96
5				98
6				96
7				93

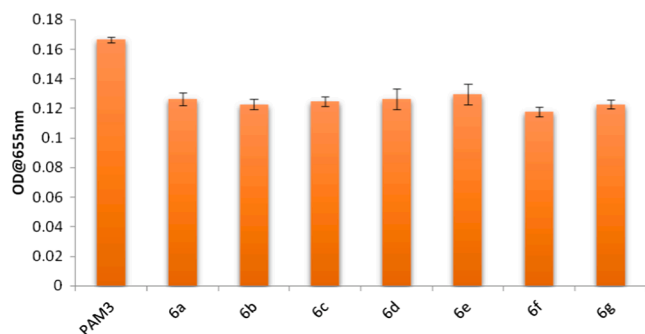


Fig. 3. Human TLR-2 SEAP assay. HEK-Blue™ hTLR2 cells were accelerated with agonists: Pam₃CysSK₄, 6a, 6b, 6c, 6d, 6e, 6f and 6g (10 μg/ml). After 24 h incubation SEAP activity was determined using QUANTI-Blue™ reading OD at 655 nm.

3.2.2. Cytotoxicity assay

All new Pam₃CAG conjugates were tested for their possible cytotoxicity on splenocytes and the observed % proliferation of immune cells after treatment with different doses of these analogs was quite impressive (Fig. 4), indicative of their nontoxic nature. Both B-lymphocyte and T-lymphocyte proliferation was quantified after re-stimulation with LPS and ConA.

3.2.3. Th1 and Th2 cytokines

Cytokine estimation was done by sandwich ELISA. Bar representation in Fig. 5 shows that these analogs of Pam₃CAG help immune cells to release IL-6 and TNF-α cytokines, thus representing both Th1 and Th2 response. Th1 covers TNF-α cytokines whereas Th2 response covers IL-6.

3.2.4. Antigen specific IgG titer

Post antigen challenge serum IgG estimation was done by indirect ELISA. From the Figure it is clear that 6e and 6f analog of Pam₃CAG at concentration 20 and 30 μg/dose respectively showed higher HBsAg antigen specific IgG titer against the standard TLR2 agonist

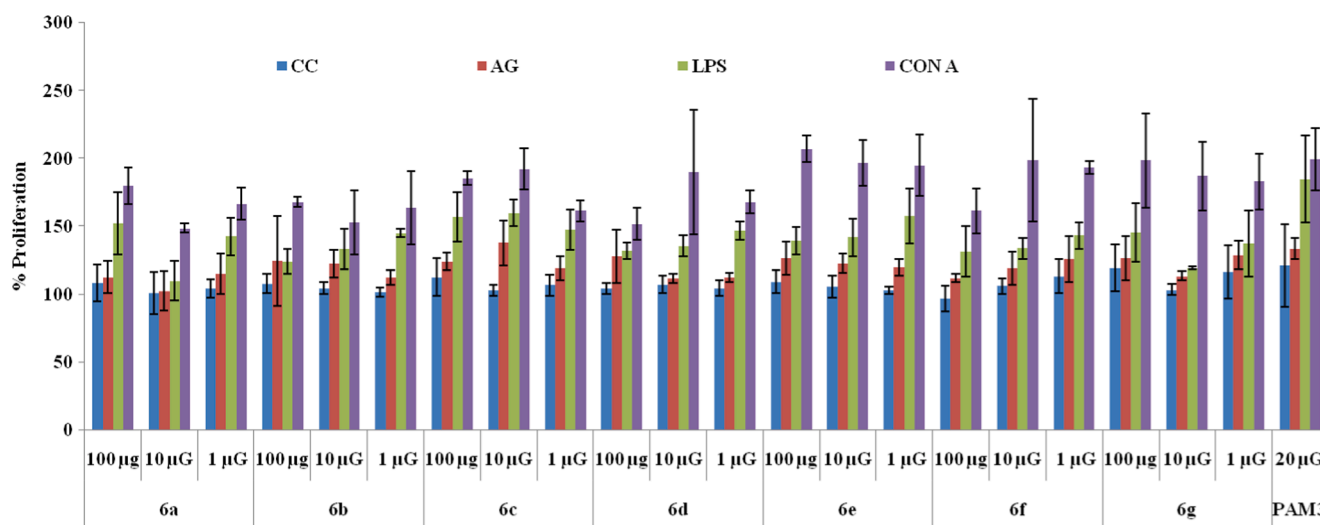


Fig. 4. Cytotoxicity effect of Pam₃CysSK₄ (20 μg) and 6a, 6b, 6c, 6d, 6e, 6f, 6g at 1, 10, 100 μg each on spleen cells. After 48 h incubation the OD was observed at 630 nm.

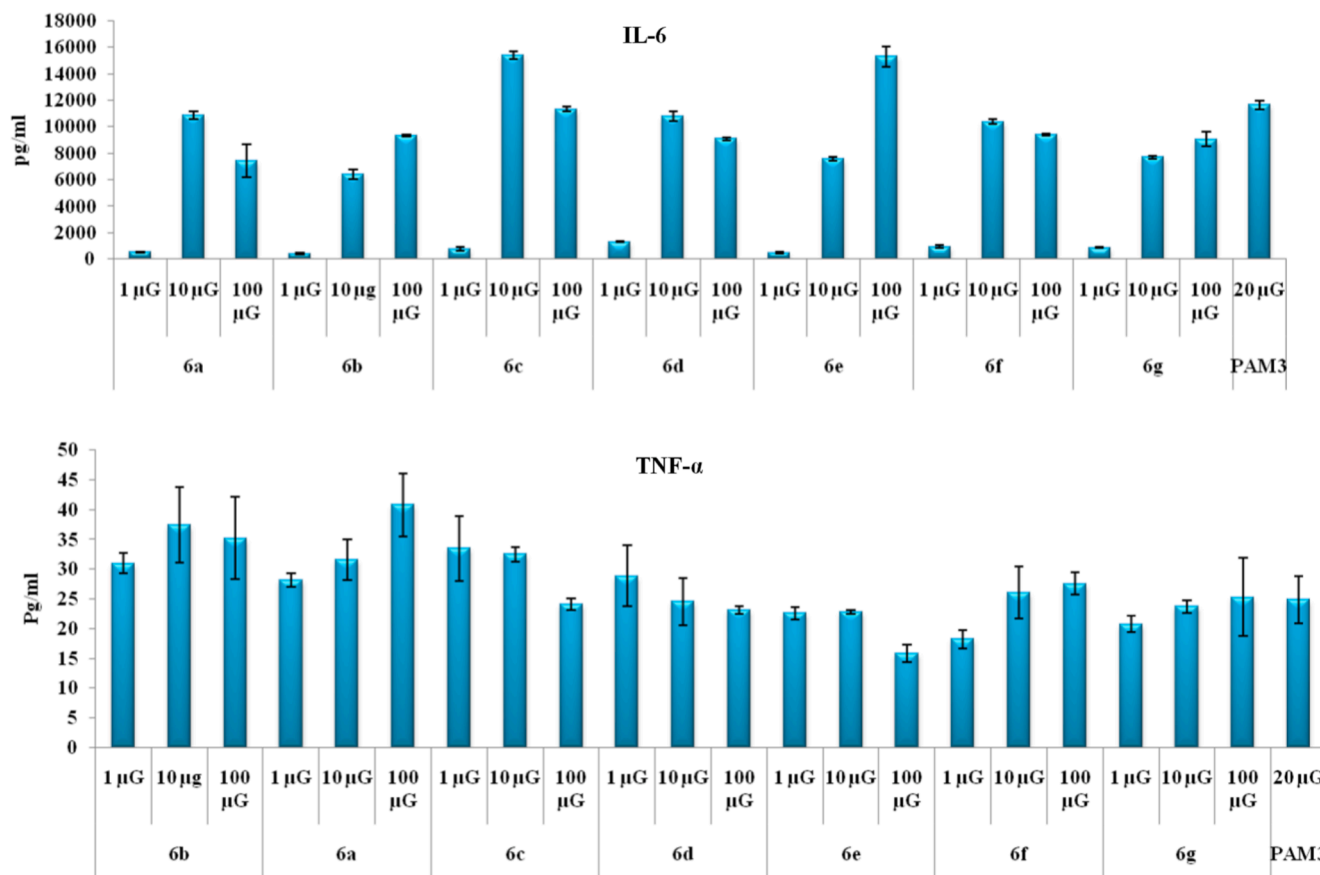


Fig. 5. Serum cytokine estimation @450 nm. BALB/c mice were immunized with ova albumin Ag (100 µg) restimulated with Pam₃CysSK₄ (20 µg) and analogs 6a, 6b, 6c, 6d, 6e, 6f at 1, 10, 100 µg each.

Pam₃CysSK₄, as compared to other test compounds. However, most of the analogues exhibited equally better IgG response compared to antigen alone groups (Fig. 6). Thus, the compounds which showed good IgG response were taken forward for further studies.

3.2.5. Immunophenotyping

To check the immune response evoked by the 6e and 6f analogs of

Pam₃Cys quantification of CD4 and CD8 markers was done by using flow cytometer. To quantify the markers, splenocytes so isolated were labeled with fluoro-chrome antibodies i.e. FITC-A antiCD4 and APC-Cy7-A antiCD8. Lymphocytes were gated and markers were estimated proving that these analogs have significantly given both humoral and cell mediated immunity. Data shown in Fig. 7 clearly mentioned the % of CD4 cells which are responsible for humoral or antibody-dependent

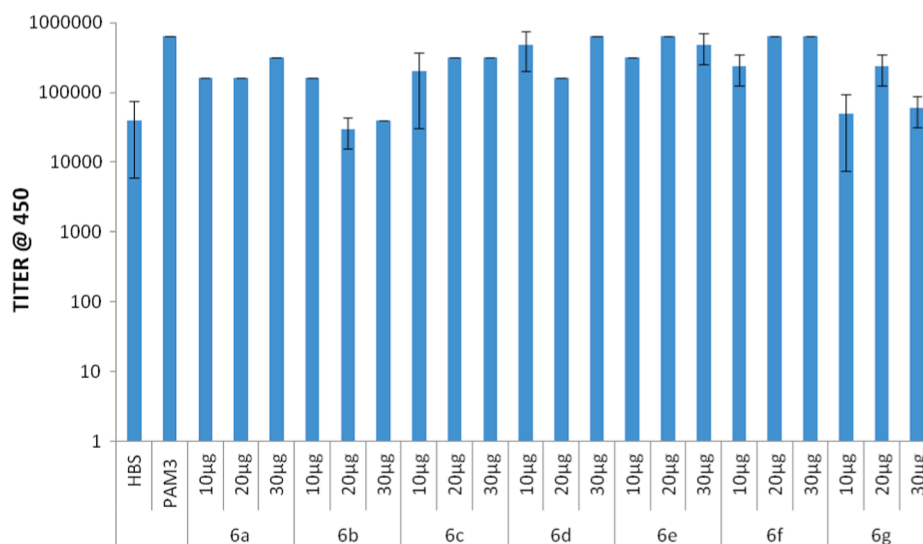


Fig. 6. Total Ig G measurement from the treated mice sera. BALB/c mice were immunized with HBS Ag (1 µg) alone or in combination with Pam₃CysSK₄ (20 µg), 6a, 6b, 6c, 6d, 6e, 6f, 6g at 10, 20, 30 µg each @450 nm.

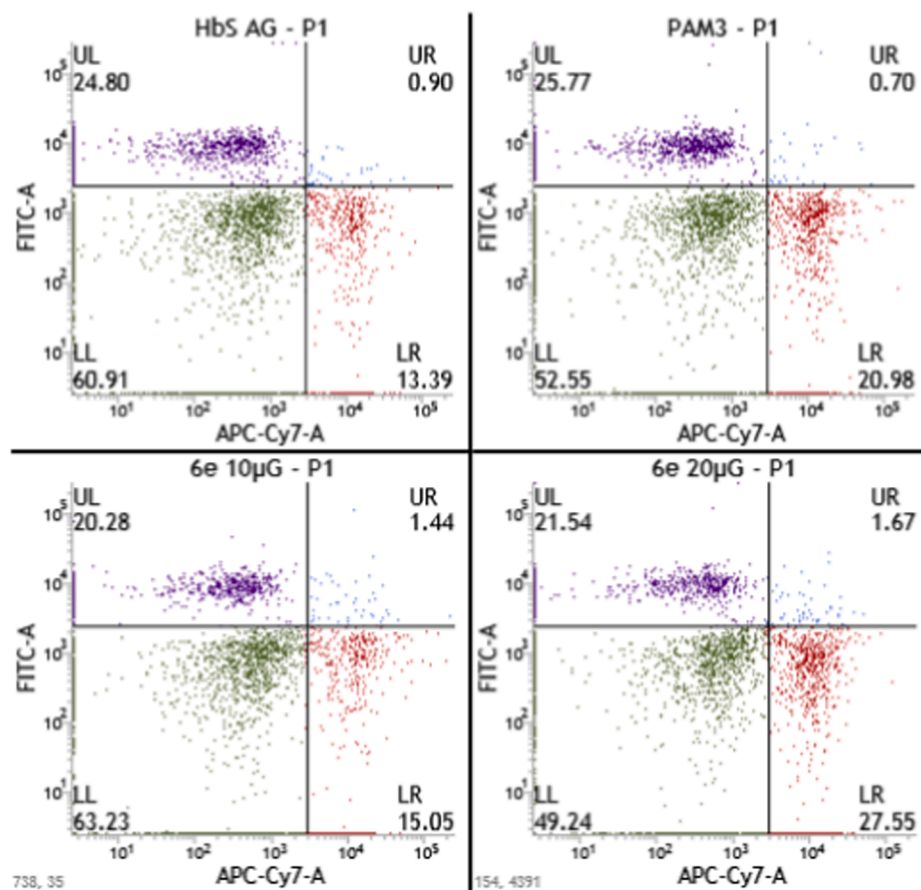


Fig. 7. T cell stimulation by cell surface markers. BALB/c mice were immunized with HBS Ag (1 μ g) alone or in combination with Pam₃CysSK₄ (20 μ g), 6e, 6f at 10, 20, 30 μ g each. Staining of spleen cells (3X10⁵cells/FACS tubes) with T cell surface marker FITC-A antiCD4 and APC-Cy7-A antiCD8.

immunity thus activating Th cells and antigen presenting cells. Apart from CD4 cells, CD8 cells were also quantified which are responsible for cell mediated immunity. Both the groups were more and the less maintained at the same level thus giving a clear correlation of antigen cross presentation.

3.2.6. Splenocyte proliferation by MTT assay

Splenocyte proliferation was done by MTT assay. The cells were restimulated with HBsAg, LPS and ConA. After 48 h incubation MTT reagent was added for the quantification of proliferation of splenocyte. The results displayed in Fig. 8 shows that 6e and 6f group shows potent proliferation when compared to that of standards (Pam₃CysSK₄ and HBsAg).

3.2.7. DC activation- surface marker estimation

From the data it is clear that compound 6e has elicited significant MHC II expression when compared to that of the standard Pam₃CysSK₄ (Fig. 9).

3.3. In silico studies

The docking showed that all the ligands are effectively with TLR1-TLR2 complex as it is clearly evidenced from their XP score. The residues 256, 258, 261, 266, 269–70, 273–74, 279, 282–84, 289, 293–95 (hydrogen bonding sites) and 304–29, 331–41, 343, 346–52, 355, 359, 367, 370–71, 376 (as hydrophobic pocket) were selected for the Prime Refinement stage. Especially Hydrogen bond forming amino acid residues were considered to be most crucial for the docking. Total 2279 binding poses were analyzed for the best ligand 6e, 6f and 6d out of the

designed ligand set its has been found that in 6a–d showed interactions Tyr335 with triazolyl centre, Gly313, Asp, 327, leu 330, lys437, phe 325, proline 352 and 6e–f Asp327 triazolyl, val311, gln316, leu350, phe349 hydrogen bond. The table IFD docking represents three stage of the docking algorithm used for the study. (i) surface docking of mono-chain insertion in TLR1; (ii) Di-leg insertion in TLR2 and; (iii) three leg insertion in TLR2-TLR1 complex. Though the results obtained are deviated from their biological behaviour Figs. 10 and 11.

Binding affinities prediction for of the full series PamCysSK₄ analogues was obtained explaining the TLR specificity assay (RMSD). By comparison, the best model obtained where the two charged ligands (6a and 6g) were omitted is only somewhat better with a RMSD of 0.872 kcal/mol. This is probably a result of the knowledge of the initial docked position from the crystal structures. Using this technique, we also investigated different combinations of protein charged states and electrostatic cutoffs. The best comparison was obtained using a charged residue shell of 9.6 Å around the ligand in combination with a 15 Å residue-based electrostatic cutoff. The robustness of the results is well-illustrated by the 1.355 kcal/mol RMSD obtained using the leave-one-out cross validation technique. This indicates that the fit is not biased by any particular ligand. It is well evidenced that 6e and 6f shoed –1143.20 and –1138.64 kcal/mol. Therefore to inspect further we performed docking with TLR1 and TLR2 individually and the $\Delta\Delta G_{binding}^{TLR1-TLR2}$ calculated by subtracting the $\Delta G_{binding}^{TLR1} + \Delta G_{binding}^{TLR2}$ from $\Delta G_{binding}^{TLR1-TLR2}$ it was found that 6e and 6f showed favourability for the formation of the stabilised complex.

The MM/PBSA studies disclosed that 6e and 6f interacted TLR1-TLR2 complex with $\Delta G_{binding}$ –3764.79 and –4469.43 kcal/mol

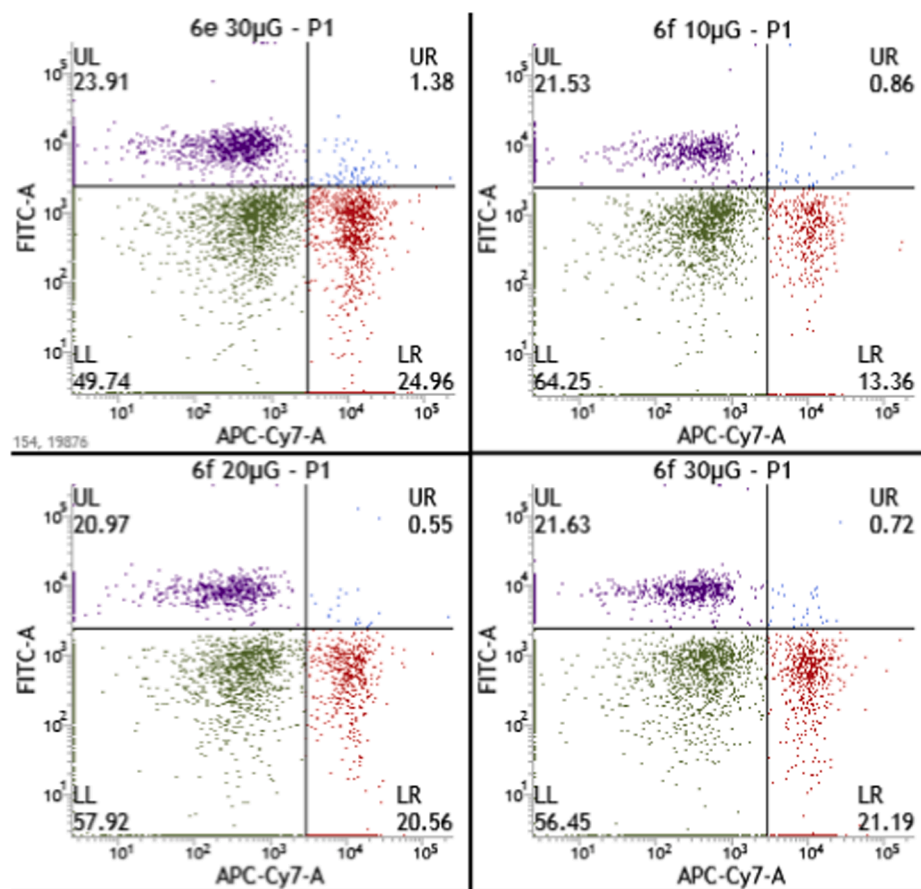


Fig. 7. (continued).

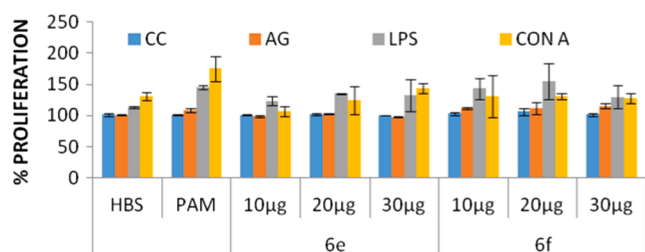


Fig. 8. % proliferation of splenocytes @630 nm. BALB/c mice were immunized with HBS Ag (1 µg) alone or in combination with Pam₃CysSK₄ (20 µg), 6e, 6f at 10, 20, 30 µg each. The cells were re-stimulate with HBS Ag, LPS and CON A at 0.1, 10 and 2 µg/ml respectively.

though the values are lower than the standard ligand which showed very high $\Delta G_{\text{binding}}$ of -1054 kcal/mol due to the high number of hydrogen bonding site offering more stable Protein-ligand complex.

4. Discussion

Even though commercially available standard TLR2 agonists like Pam₃CysSK₄ show potential adjuvant activity, their actual usefulness with various unconjugated antigens in vaccine formulations has been severely limited which is most likely attributed to its polycationic nature. Even though other TLR2 agonist Pam₃CAG is known to be promising ligand that induce DC maturation and B cell proliferation *in vitro*, it is more suitable for liposomal formulations as evidenced in case of Pam₃CAG-PEG conjugates. Undoubtedly, suitable analogues of Pam₃CAG fine tuned HLB, suitable for *in vivo* application with exogenous subunit antigen such as HBsAg is highly needed. Covalently conjugating

hydrophilic alcohols with Pam₃CAG is an interesting option to modulate the overall HLB of the conjugate, to make them suitable for use as adjuvants with subunit antigens. Azide-alkyne click chemistry is an attractive and convenient tool to tether together both these entities through a triazolyl spacer, enabling high yields of the desired conjugates with complete regioselectivity. A focused library of seven novel conjugates of Pam₃CAG were synthesized and tested for their immunogenicity as vaccine adjuvants against HBsAg.

First of all, the focused library was subjected for mechanistic studies to check the target specificity against TLR-2. When compared to standard Pam₃CysSK₄, it was found that all the compounds were acting as a potential ligand for TLR-2. In *ex vivo* studies, the foremost thing was to check the cytotoxicity of the compounds. The mice were immunized with ovalbumin (100 µg) on 0th day and finally sacrifices on 7th day for spleen collection. The splenocytes were restimulated with ova albumin alone or in combination with Pam₃CysSK₄, analogs (6a, 6b, 6c, 6d, 6e, 6f), LPS and CON A. The results derived after 48 h incubation proves that these compounds are non-toxic in nature, interestingly these compounds were proliferating splenocytes. Splenocyte proliferation was further confirms by cytokine estimation. Both Th1 and Th2 cytokines were estimated from the cell culture supernatant. Previous studies indicates that IL-6 and TNF- α are the signature cytokines for Pam₃CysSK₄, so were considered for study [41]. The cytokine profile of the test compounds at different doses is given in Fig. 5 which is indicative of their capability to induce both IL6 and TNF- α , as modulator of Th1/Th2 cytokine expression to varying levels. IL-6 being a pro-inflammatory cytokine, helps in inflammation along with maturation of B-cells. Generally it is secreted at sites of acute and chronic inflammation inducing transcriptional inflammatory response via IL-6 receptors (CD126). TNF- α , an inflammatory cytokine is generally produced by the action of macrophages or monocytes at the site of acute inflammation.

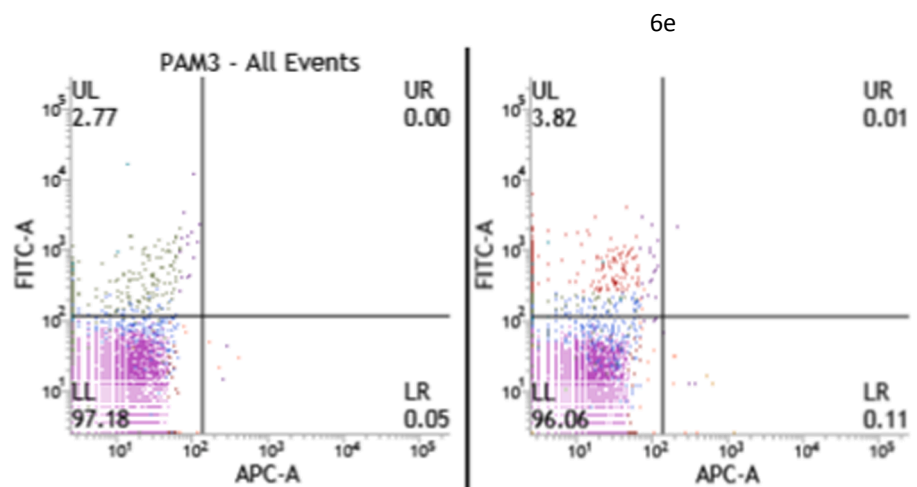


Fig. 9. DC stimulation by cell surface markers. BALB/c mice were sacrificed and splenocytes isolated were treated with Pam₃CysSK₄ and compounds **6e** at 20 µg concentration each for 24 h. Staining of spleen cells (3×10^5 cells/FACS tubes) with cell surface marker FITC-A anti MHC II and APC-A anti CD86.

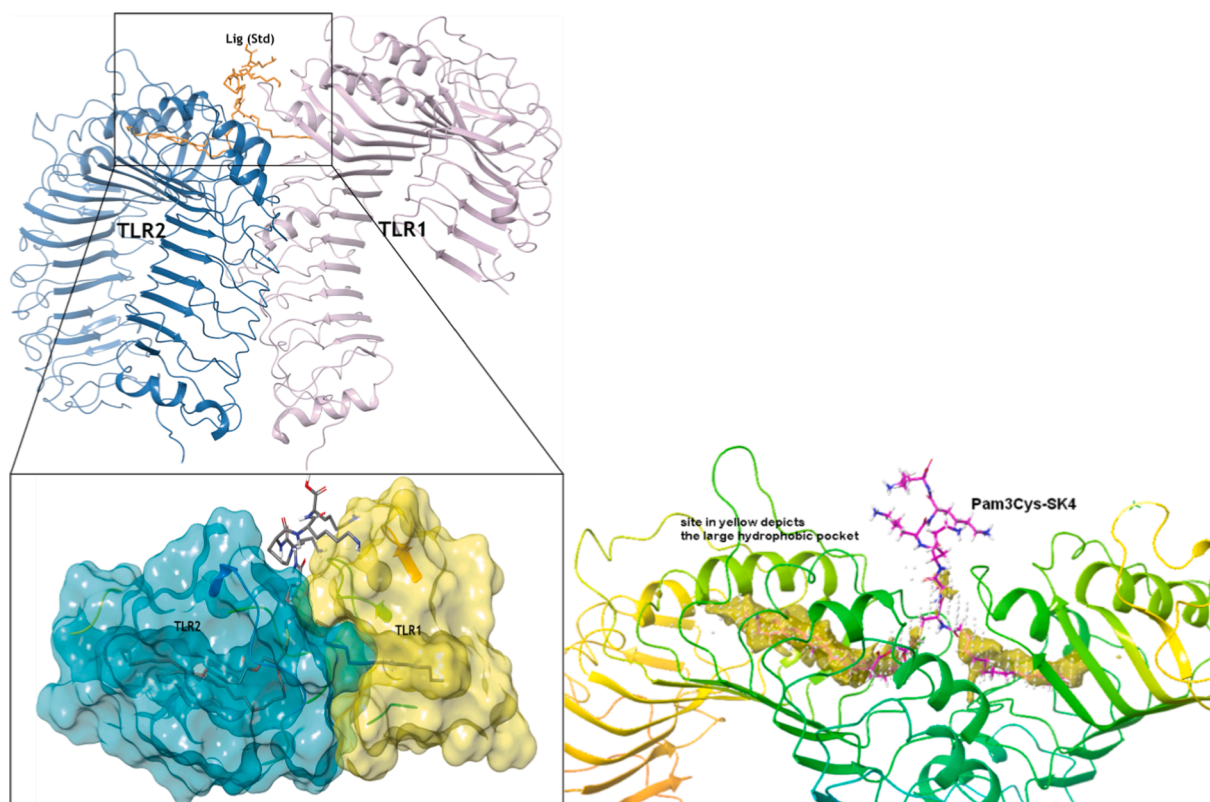


Fig. 10. Crystal structure of TLR1-TLR2 with Pam₃CysSK₄ and depiction of legs of the ligand with TLR1-TLR2 complex.

TNF- α exhibit a disparate dimension of signaling actions within cells which ultimately leads to necrosis or apoptosis.

Encouraging results from *ex vivo* analysis made us to take it further *in vivo* analysis. Mice were immunized in different groups with varying concentrations of test compounds along with HBsAg antigen using standard adjuvant Pam₃CysSK₄ as reference standard. All the test groups (HBsAg, Pam₃CysSK₄, **6a**, **6b**, **6c**, **6d**, **6e**, **6f** and **6g**) were analyzed for HBsAg specific IgG response. IgG is a dominating class of immunoglobulin found in blood serum covering approximately 75% of total serum immunoglobulins. The production of IgG indicates the secondary immune response against the antigen. Thus IgG response is a principal tool for evaluating the quality of host immune response to a vaccine.

Estimation of humoral response by ELISA revealed dose dependent enhancement in IgG response and amongst all the test compounds, only two analogues **6e** and **6f** shown significant response when compared with standard adjuvant. Thus compound **6f** at concentration 20 µg and **6e** at concentration 30 µg exhibited almost equal response when compared to that of standard adjuvant Pam₃CysSK₄.

Immunophenotyping of splenocytes upon treatment with varying doses of test compound **6e** and **6f** exhibited dose dependent improvement in CD4 and CD8 populations compared to standard adjuvant Pam₃CysSK₄ or antigen (HBsAg alone) with compound **6e** enhancing CD8⁺ population markedly at 20 µg concentration (**2e**, 27.55% > Pam₃CysSK₄ + HBsAg, 20.99% > HBsAg, 13.39%) which confirm that

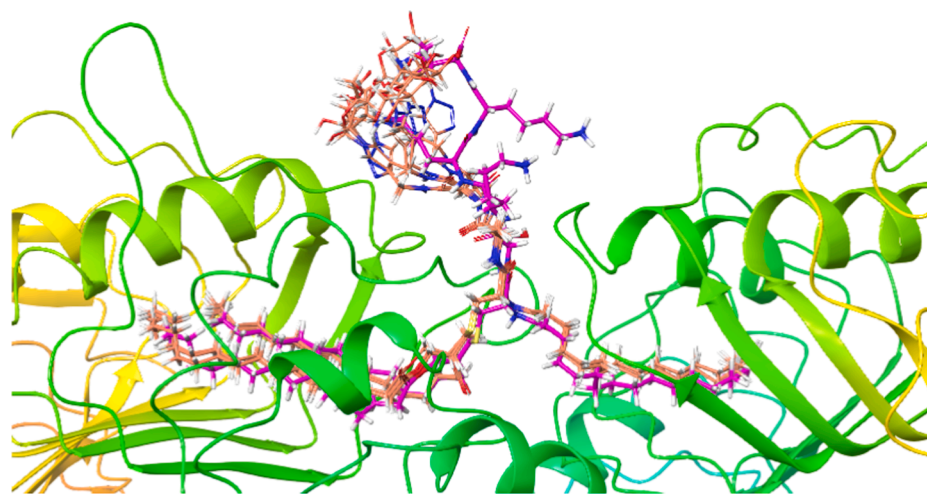


Fig. 11. The IFD results obtained and their superimposition (6d and 6f).

predominant cell mediated response, even though the corresponding CD4+ response was slightly lower compared to standard adjuvant Pam₃CysSK₄ (Pam₃CysSK₄ + HBsAg, 25.77 > 2e, 23.91% at 30 µg). CD8 cells contribute to adaptive immunity, crucial for surmounting cytotoxic T-lymphocyte response against intracellular pathogens like viral infections whereas, CD4 are the surface markers present on Th cells which stimulates antigen presenting cells like B-cells, macrophages including CD8 T lymphocytes, thus coordinating the adaptive immune response. Enhanced antibody response upon compound (6e) treatment along with HBsAg at 20 µg concentration reveal that the observed stimulation of CD4 is sufficient enough to evoke effective humoral immunity. Thus both CD4 and CD8 play crucial role in inducing quality immune system required for pathogen clearance. *Ex vivo* estimation of MHC class-II expression on isolated DCs, upon compound treatment, indicated significant enhancement in MHC-II expression (3.82%, 20 µg of 6e) compared to standard adjuvant (Pam₃CysSK₄ + HBsAg, 2.77%).

LPS and CON-A are standard mitogens for B and T cell proliferation. When selected groups administered with test compounds in different doses, were restimulated with HBsAg, LPS and CON-A, the % proliferation of cells in MTT assay showed potential proliferation of B and T cells without any cytotoxicity. A, but test compound 6e (at 30 µg) and 6f (at 20 µg) showed significant proliferation. Both B-cell proliferation and T-cell proliferation is essential to fight any kind viral and bacterial infections. B-cells not only produce antibodies against that particular pathogen but also retain the memory for further defense from the particular pathogen.

5. Conclusion

Our TLR-2 functional bioassay determined that novel Pam₃CAG analogues presented here had human TLR-2 agonistic activity comparable to those of the reference compound Pam₃CysSK₄. The novel Pam₃CAG conjugates, show activities of different magnitude indicating the modulation of immune response by different substitution with varieties of sugars and alcohols. Based on the immune response derived, it could be inferred that the number of hydroxyl groups present on the scaffold on substitution "R" is playing a significant role rather than the cyclic or acyclic nature of the substitution. Thus, the substituent with two and three hydroxyl groups exhibited optimal immune response compared to substituent with lesser (one hydroxyl) or more than three hydroxyls. Compounds 6e and 6f demonstrated significant enhancement of OVA and HBsAg specific IgG response. Both the analogues showed marked improvements in CD4 and CD8 surface markers expression, a hall mark of enhanced Th and cell mediated immunity, indicating their usefulness in vaccines against intracellular pathogenesis. Thus the new triazole

tethered Pam₃CAG conjugates exhibited their capability to potentiate both humoral and cell mediated immune response, demonstrating their usefulness as vaccine adjuvants.

6. Experimental section

6.1. Chemistry

6.1.1. Synthesis of (R)-3-((S)-3-oxo-3-(2-oxo-2-phenylethoxy)-2-palmitamidopropylthio) propane-1,2-diyl dipalmitate (S5)

The diol compound S4 [32] (3.01 g, 7.28 mmol) was dissolved in dry THF and palmitic acid (5.59 g, 21.8 mmol), DIC (3.6 g, 27.9 mmol), DMAP (0.35 g, 2.9 mmol), were added one after another under inert atmosphere. This reaction mixture was allowed to stir for 4 h at room temperature. After complete consumption of starting material solvent was evaporated under reduced pressure to furnish semi solid residue which was used further without purification. This obtained residue (6 g, 6.74 mmol) was dissolved in 20% TFA: CH₂Cl₂ and stirred at room temperature for 40 min. After completion of starting material excess solvent was evaporated by rota vacuo. Residue co-evaporated with hexane, then subjected to azeotropic evaporation with toluene and the residue obtained was used in the next step. Resulting amine compound (5.32 g, 6.7 mmol) was dissolved in dry THF and the solution was added to previously stirred solution of the palmitic acid (2.05 g, 8.04 mmol), DIC (1.03 g, 8.04 mmol), HOBt (1.23 g, 8.04 mmol) in dry THF. After addition, reaction mixture was stirred at room temperature for 5 h. After completion of starting material reaction mixture was diluted with ethyl acetate, washed with water (50 ml), satd NaHCO₃ (50 ml). The aqueous layer extracted with ethyl acetate (20 ml). The combined organic layers were dried over anhydrous Na₂SO₄ and the solvent was evaporated under vacuum to afford the impure residue. The residue was purified by column chromatography from using 35% Ethyl acetate/hexane as eluent to give compound S5 as light yellow solid (4.9 g, 60% over three steps). ¹H NMR (300 MHz, CDCl₃) δ 7.90 (d, J = 7.5 Hz, 2H, aromatic), 7.62 (t, J = 7.4 Hz, 1H, aromatic), 7.49 (t, J = 7.6 Hz, 2H, aromatic), 6.43 (dd, J = 18.2, 7.6 Hz, 1H, -NH), 5.50 (d, J = 16.3 Hz, 1H, phenacyl-CH₂-), 5.35 (d, J = 16.4 Hz, 4H, Phenacyl-CH₂-), 5.26 – 5.13 (m, 1H, -CH-O ester), 4.96 (dd, J = 12.1, 6.4 Hz, 1H, α-CH-of cys), 4.35 (dd, J = 11.7, 3.4 Hz, 1H, -CH₂-O ester), 4.16 (dd, J = 11.7, 3.4 Hz, 1H, -CH₂-O ester), 3.27 (dd, J = 13.9, 4.8 Hz, 1H, -S-CH₂-), 3.12 (dd, J = 14.0, 6.5 Hz, 1H, -S-CH₂-), 2.81 (d, J = 6.4 Hz, 2H, -CH₂-S-), 2.30 (dt, J = 16.1, 7.9 Hz, 6H, α-CH₂-C=O-), 1.61 (m, 1.70–1.53, 6H, β-CH₂-C=O-), 1.25 (bs, 76H, -CH₂-lipid chains), 0.87 (t, J = 6.4 Hz, 9H, 3-CH₃ lipid chains); ¹³C NMR (101 MHz, CDCl₃) δ 191.27 (-C=O phenacyl ring), 173.40 (-C=O palmitoyl ester), 173.31 (-C=O palmitoyl ester), 173.16 (-C=O

phenacyl ester), 170.49(NH—C=O palmitoyl amide), 134.15(aromatic), 133.89(aromatic), 128.99(aromatic), 127.78(aromatic), 70.31(—CH— ester), 66.78(α -CH₂-phenacyl), 63.63(—CH₂-O-ester), 51.84(α -CH-cysteine), 36.40(—CH₂-S-), 34.65(S-CH₂-), 34.34(α -CH₂- of palmitoyl amide), 34.12(α -CH₂- of palmitoyl ester), 32.98(α -CH₂- of palmitoyl ester), 31.96, 29.74, 29.56, 29.40, 29.18, 25.56, 24.96, 24.91, 22.72, (31.96 to 22.72 methylene carbons of lipids), 14.15(—CH₃ of lipids); **LRMS**: Calculated for C₆₂H₁₀₉NO₈S 1027.78; Found: 1050.7797 [M + Na]⁺.

6.1.2. Synthesis (S)-3-((R)-2,3-bis(palmitoyloxy)propylthio)-2-palmitamidopropanoic acid (2)

Compound **S5** (4.9 g, 4.7 mmol) was dissolved in glacial acetic acid (50 ml) and activated Zn (4.95 g, 76.2 mmol) was added to it at room temperature. Reaction mixture was stirred for 2 h at same temperature. After complete consumption of the starting material, the reaction mass was filtered through celite. The filtrate was evaporated under reduced pressure to afford crude product. This crude product was subjected to purification by column chromatography, using 50–80% EtOAc/Hexane as eluent to afford pure compound **2** (3.89 g, 90%) as white solid, mp 63–65 °C. ¹H NMR (400 MHz, CDCl₃) δ 6.58 (d, 7.2 Hz, 1H, —NH), 5.15 (qd, J = 6.4, 3.5 Hz, 1H, —CH-O ester), 4.77 (ddd, J = 15.8, 11.9, 5.8 Hz, 1H, α -CH Cys), 4.38–4.31 (m, 1H, —CH₂-O ester), 4.17–4.08 (m, 1H, —CH₂-O ester), 3.19–2.99 (m, 2H, S-CH₂-cys), 2.80–2.68 (m, 2H, —CH₂-S-), 2.35–2.24 (m, 6H, α -CH₂ of lipid chains), 1.69–1.52 (m, 6H, β -CH₂ of lipid chains), 1.25 (bs, 72H, —CH₂- lipid chains), 0.87 (t, J = 6.8 Hz, 9H, 3-CH₃ lipid chains); ¹³C NMR (126 MHz, CDCl₃) δ 174.49(—C=O of acid), 174.29(—C=O ester), 173.64(—C=O ester), 172.70(—C=O amide) 70.24(—CH-O ester), 63.70(—CH₂-O ester), 52.10(α -CH Cys), 51.93(—CH₂-S-), 36.35(α -CH₂ amide), 36.31(S-CH₂-), 34.37(α -CH₂- ester), 34.13(α -CH₂- ester), 32.97, 31.96, 29.75, 29.70, 29.57, 29.40, 29.34, 29.17, 25.57, 24.96, 24.90, 22.72, (32.97 to 22.72 —CH₂- of lipid chains) 14.14(—CH₃ of lipids); **LRMS**: Calculated for C₅₄H₁₀₃NO₇S 909.7455; Found: 932.50 [M + H]⁺.

6.1.3. Synthesis of (R)-tert-butyl (1-oxo-1-((2-oxo-2-(prop-2-yn-1-ylamino)ethyl)amino)propan-2-yl)carbamate (3)

Compound **3** (Boc-Ala-Gly-OEt) was synthesized from Boc-Alanine and ethyl glycinate. EDC.HCl (30 g, 158 mmol) and HOBt (21.42 g, 158 mmol) were added to a solution of Boc-Ala-OH (25 g, 132.0 mmol) dissolved in dry DMF. This reaction mixture was stirred for 15 min then HCl.NH₂-Gly-OEt (18.5 g, 132.0 mmol) and DIPEA (29 ml, 264.0 mmol) were added. The mixture was stirred at room temperature for 8 h. After complete consumption of starting material, reaction was quenched with addition of ice cold water. Ethyl acetate was added to this solution and extracted with it. The organic layer was washed with 5% sodium bicarbonate and water. The organic layer was dried with anhydrous sodium sulfate, was concentrated to dryness to get an oily residue of compound **3**. This was purified by column chromatography (2:98 CH₃OH:CHCl₃) (25.37 g, 70% yield). ¹H NMR (400 MHz, DMSO-*d*₆) δ 8.16 (t, J = 5.8 Hz, 1H, Gly-NH), 6.92 (d, J = 7.6 Hz, 1H, Ala-NH), 4.08 (q, J = 7.1 Hz, 2H, —OCH₂CH₃), 3.99 (dd, J = 14.4, 7.1 Hz, 1H, α -H of ala), 3.81 (ddd, J = 37.3, 17.4, 5.9 Hz, 2H, —glycine-CH₂), 1.37 (s, 9H, Boc), 1.21–1.15 (m, 6H, —OCH₂CH₃ and —CH₃ of Ala), ¹³C NMR (75 MHz, DMSO-*d*₆) δ 173.16 (>C=O ala), 169.60(>C=O gly), 154.87(—CO Boc), 79.05(>C < of Boc), 77.88, 60.23(O-CH₂CH₃), 49.36(α -CH of ala), 40.56(α -CH₂ of gly), 28.08(3 —CH₃ of *t*-butyl), 18.07(β -CH₃ ala), 13.93(O-CH₂CH₃); **LRMS**: Calculated for C₁₂H₂₂N₂O₅ 274.3134; Found: 297.25 [M + Na]⁺.

6.1.4. Synthesis of compound 4

Lithium hydroxide (1.312 g, 54.66 mmol) was added portion wise to a solution of compound **3** (10 g, 36.44 mmol) in MeOH: Water (60 ml, v/v) at 0 °C. Then reaction mixture was allowed to stir at RT for 2hrs. After complete consumption of starting material, reaction mixture was diluted with EtOAc (30 ml) and water (20 ml). Basic P^H was adjusted upto 3 by

adding saturated citric acid. Organic layer was separated and aqueous layer was extracted (3 × 30) with ethyl acetate. Combined organic layer was dried over Na₂SO₄ and concentrated under reduced pressure to give crude Boc-Ala-Gly-OH. This acid compound (9.48 g, 36.44, 100%) was directly used for next reaction. EDC.HCl (10.44 g, 54.68 mmol) and HOBt (3.69 g, 27.34 mmol) were added to a solution of crude acid compound (4.74 g, 18.22 mmol) dissolved in 100 ml dry THF. Resulting mixture was stirred for 30 min at ambient temperature. After 30 min of stirring, reaction kept at 0 °C and propargyl amine (2.80 ml, 43.72 mmol), DIPEA (12.59 ml, 72.88 mmol) in 20 ml dry THF were added slowly to the above reaction mixture. Reaction was allowed to stir at ambient temperature for 10 hrs. After completion of reaction, water (50 ml) and EtOAc (50 ml) were added. Aqueous layer was separated and organic layer was washed with brine (25 ml) and sat NaHCO₃ (30 ml). Organic layer was dried over Na₂SO₄ and concentrated under reduced pressure. Crude product **4** was purified by column chromatography using 2%CH₃OH:CHCl₃ as eluent. Yield: 85% (8.81 g) White solid MP-149–151 °C; ¹H NMR (400 MHz, CDCl₃) δ 7.02 (bs, 1H, —NH), 6.83 (bs, 1H, —NH), 5.06 (d, J = 5.8 Hz, 1H, —NH), 4.14–3.89 (m, 5H, α -CH of ala, α -CH₂ and —C=ONHCH₂-of gly), 2.20 (t, J = 2.5 Hz, 1H, alkyne-CH), 1.45 (s, 9H, Boc), 1.38 (d, J = 7.1 Hz, 3H, —CH₃ of ala); ¹³C NMR (100 MHz, CDCl₃) 174.28(C=O of ala), 169.26(C=O of gly), 156.13(C=O of Boc), 79.92(>C < of Boc), 78.68(alkyne -C-), 70.78(alkyne-CH) 50.40(α -CH of ala), 42.06(α -CH₂ of gly), 29.20, 28.33, 27.75(Boc-CH₃), 16.93(—CH₃ of ala); **HRMS (ESIMS)** calcd. for C₁₃H₂₁N₃O₄ [M + Na]⁺: calcd. *m/z* 306.1430; found: 306.1435

6.1.5. Synthesis of (9R,12S,16R)-9-methyl-5,8,11-trioxo-12-palmitamido-14-thia-4,7,10-triazaheptadec-1-yne-16,17-diyldipalmitate (5)

To a solution of Compound **2** (Pam₃Cys-OH, 5 g, 5.49 mmol) in 50 ml dry THF under N₂ atmosphere were added EDC.HCl (1.57 g, 8.23 mmol) and HOBt (1.11 g, 8.23 mmol). This reaction mixture was allowed to stir for 30 min at RT. Meanwhile compound **4** (0.605 g, 11 mmol) was treated with 20%TFA: DCM (20 ml) for 40 min and this reaction mixture concentrated and treated with DIPEA (3.82 ml, 21.96 mmol) at 0 °C in dry THF. This was added to the above reaction mixture of acid at 0 °C. The resulting reaction mixture was allowed to stir overnight. After the completion of reaction, CH₂Cl₂ (50 ml) was added to it. The organic layer was washed with water (2 × 50 ml) and saturated NaHCO₃ (2 × 50 ml), dried over Na₂SO₄ and organic solvent was removed under vacuum. The crude residue was purified by column chromatography (2% MeOH: Chloroform) to obtain required compound **5** in good yield (4.14 g, 70%) as white solid. mp 145.0 °C; ¹H NMR (300 MHz, CDCl₃ + CD₃OD) δ 5.18–5.09 (m, 1H, —CH-O ester), 4.47 (t, J = 6.9 Hz, 1H, α -CH-cys), 4.39–4.20 (m, 2H, α -CH-ala, CH₂-O ester), 4.08 (dd, J = 12.0, 6.5 Hz, 1H, —CH₂-O ester), 3.95 (dd, J = 4.1, 2.4 Hz, 2H, —CH₂-gly), 3.83 (d, J = 13.1 Hz, 2H, —CH₂-propargyl), 2.93 (dd, J = 13.5, 6.5 Hz, 1H, S-CH₂-), 2.80 (dd, J = 13.8, 7.2 Hz, 1H, S-CH₂-), 2.75–2.64 (m, 2H, —CH₂-S-), 2.33–2.14 (m, 7H, alkyne-CH, α -CH₂ lipid chains), 1.64–1.45 (m, 6H, β -CH₂-lipid chains), 1.35 (d, J = 7.2 Hz, 3H, —CH₃ alanine), 1.20 (bs, 70H, —CH₂-lipid chains), 0.82(t, J = 6.4 Hz, 9H, 3-CH₃ lipid chains); ¹³C NMR (75 MHz, CDCl₃ + CD₃OD) δ 174.46(—C=O ester), 173.61(—C=O ester), 173.54(—NHC=O, palmitoyl) 172.85(—NHC=O peptide), 171.10(—NHC=O peptide), 169.06(—NHC=O peptide), 79.04(alkyne C), 70.95(—CH-O ester), 70.06(terminal C-alkyne), 63.58(—CH₂-O ester), 52.30(α -CH-cysteine), 49.60(α -CH-alanine), 42.18(α -CH-glycine), 35.89(—CH₂-S-), 34.06(S-CH₂-), 33.98(α -CH₂ of NHCOpalm), 33.83(α -CH₂ of COOpalm), 32.46, 31.65, 29.41(—NHCH₂-propargyl), 29.25, 29.08, 28.86, 28.55, 27.51, 25.31, 24.67, 24.60, 22.39, 21.17, (32.46 to 21.17, —CH₂- lipid chains), 16.58(β -CH₃ alanine), 13.71(—CH₃ lipid chains); **HRMS (ESIMS)** calcd. for C₆₂H₁₁₄N₄O₈S [M + Na]⁺: calcd. *m/z* 1097.8255; found: 1097.8274

6.1.6. General procedure for the synthesis of 1, 2, 3-triazole tethered hydroxy-Pam₃CAG hybrid conjugates (6a-g)

Compound **5** (100 mg, 0.093 mmol) and polyhydroxyl azides **I-VII**

(1.2 eq, 0.111 mmol) were suspended in ter-butanol and water (5 ml, 1:1, v/v) mixture. To the above stirred solution $\text{CuSO}_4 \cdot 5\text{H}_2\text{O}$ (47 mg, 0.186 mmol) and sodium ascorbate (36.82 mg, 0.186 mmol) were added at ambient temperature. Resulting heterogeneous mixture was allowed to stir vigorously for 8–12 h at same temperature. TLC analysis indicated complete consumption of the reactants, solvent was removed under reduced pressure and crude was diluted with EtOAc (30 ml) and water (20 ml). Organic layer was separated and aqueous layer was extracted with ethyl acetate (2 × 30). Combined organic layers were washed with brine and dried over an Na_2SO_4 . Organic layers were concentrated under vacuum to give crude product which was purified by column chromatography techniques using 5% $\text{CH}_3\text{OH}:\text{CHCl}_3$ as eluent to get corresponding 1,2,3-triazolyl Pam₃Cys-Ala-Gly hybrid conjugates in quantitative yields (90 to 98%) as white solids.

6.1.6.1. (7R,10S,14R)-7-methyl-3,6,9-trioxo-10-palmitamido-1-(1-(2S,3S,4R,5S,6S)-3,4,5-trihydroxy-6-(hydroxymethyl)tetrahydro-2H-pyran-2-yl)-1H-1,2,3-triazol-4-yl)-12-thia-2,5,8-triazapentadecane-14,15-diyl dipalmitate (6a). Compound **6a** was prepared from compound **5** (100 mg, 0.093 mmol) and 1-azido-β-D-glucose **I** (23 mg, 0.111 mmol) according to the above general procedure in good yield. (93%, 110 mg) White solid; Melting point: 190–193 °C; $^1\text{H NMR}$ (300 MHz, $\text{CDCl}_3 + \text{CD}_3\text{OD}$) δ 7.94 (s, 1H, =CH triazole), 5.52 (d, $J = 9.1$ Hz, 1H, H-1 glu), 5.17–5.07 (m, 1H, -CH-O ester), 4.50–4.31 (m, 4H, α-CH-cys, α-CH-ala and -CH₂-triazole), 4.28 – 4.07 (m, 3H, -CH₂-O ester and -CH-glycine), 3.93 – 3.68 (m, 5H, H-6, H-6, H-5, H-3 of glu, -CH-gly), 3.57–3.52 (m, 2H, H-2, H-4 glu), 2.97 – 2.68 (m, 4H, -CH₂-S- and -S-CH₂-), 2.37 – 2.05 (m, 6H, α-CH₂- lipid chains), 1.66–1.48 (m, 6H, β-CH₂- lipid chains), 1.39 (d, $J = 7.1$ Hz, 3H, β-CH₃ ala), 1.34–1.15 (m, 72H, -CH₂- lipid chains), 0.85 (t, $J = 6.5$ Hz, 9H, -CH₃ lipid chains); $^{13}\text{C NMR}$ (101 MHz, $\text{CDCl}_3 + \text{CD}_3\text{OD}$) δ 175.04(-C=O ester), 173.55(-C=O ester), 173.43 (palmNH-C=O), 171.69 (-NH-CO), 171.32(-NH-C=O), 169.92 (-NH-C=O), 144.45(>C = of triazole ring), 121.55(=CH- triazole ring), 87.72 (C-1 glu), 78.95(C-5 glu), 76.35(-CH-ester), 72.27(C-3 glu), 69.91(C-4 glu), 68.83(C-2- glu), 63.24 (-CH₂O-ester), 60.62(-C-6 glu), 52.37(α-CH- cys), 49.73(α-CH- ala), 42.33(-CH₂-gly), 42.20(-CH₂-triazole), 35.31(CH₂-S), 33.83(S-CH₂-), 33.62(α-CH₂- of NHCOpalm), 31.43 α-CH₂- of COOpalm, 29.19, 28.85, 28.63, 25.19, 24.40, 22.16 (29.19 to 22.16, -CH₂-lipid chains) 16.04(-CH₃ of ala), 13.38(β-CH₃ lipid chains); **HRMS (ESI-MS)** calcd. for $\text{C}_{68}\text{H}_{125}\text{N}_7\text{O}_{13}\text{S}$ [$\text{M} + \text{H}$]⁺: calcd. m/z 1280.9134; found: 1280.9145

6.1.6.2. (7R,10S,14R)-7-methyl-3,6,9-trioxo-10-palmitamido-1-(1-(2R,3R,4R,5R,6S)-3,4,5-trihydroxy-6-(hydroxymethyl)tetrahydro-2H-pyran-2-yl)-1H-1,2,3-triazol-4-yl)-12-thia-2,5,8-triazapentadecane-14,15-diyl dipalmitate (6b). Compound **6b** was synthesized from compound **5** (100 mg, 0.093 mmol) and 1-azido-α-D-mannose **II** (23 mg, 0.111 mmol) according to the above general procedure in excellent yield (91%, 108 mg) as white solid. Melting Point: 176–1780 °C; $^1\text{H NMR}$ (300 MHz, $\text{CDCl}_3 + \text{CD}_3\text{OD}$) δ 7.94 (s, 1H, =CH triazole), 5.52 (d, $J = 9.1$ Hz, 1H, H-1 man), 5.18–5.08 (m, 1H, -CH-O ester), 4.49–4.31 (m, 4H, α-CH-cys, α-CH-ala and -CH₂-triazole), 4.27 – 4.10 (m, 3H, -CH₂-O ester, -CH-gly), 3.92 – 3.69 (m, 5H, -CH-gly, H-5, H-6, H-3, H-6 of man), 3.61–3.50 (m, 2H, H-2 man and H-4 man), 2.96 – 2.66 (m, 4H, -S-CH₂- and -CH₂-S-), 2.36 – 2.06 (m, 6H, α-CH₂- of lipid chains), 1.66–1.47 (m, 6H, β-CH₂-lipid chains), 1.39 (d, $J = 7.1$ Hz, 3H, β-CH₃ ala), 1.23 (s, 74H, -CH₂-lipid chains), 0.85 (t, $J = 6.5$ Hz, 9H, -CH₃ lipid chains); $^{13}\text{C NMR}$ (101 MHz, $\text{CDCl}_3 + \text{CD}_3\text{OD}$) δ 174.81(C=O ester), 173.44(-C=O ester), 173.28(-NHCO palm), 173.10(-NHCO- peptide), 171.37(-NHCO- peptide), 169.68(-NHCO- peptide), 144.86(>C = triazole), 122.27(=C-H, triazole) 86.39(C-1 man), 76.18(C-5 man), 70.48(CH-O ester), 69.79(C-3man), 68.08(C-4 man), 66.54(CH₂O ester), 63.06(C-2man), 60.64 (C-6 man), 52.32(α-CH- cys), 49.41(α-CH- ala), 42.01(-CH₂-triazole & gly), 35.09(CH₂-S), 33.54(S-CH₂-), 33.34(α-CH₂- of NHCOpalm), 31.32 (α-CH₂- of COOpalm), 31.20(α-CH₂- of COOpalm), 28.96, 28.84, 28.63,

28.39, 25.01, 24.19, 21.91(28.96 to 21.91, -CH₂- lipid chains), 15.78 (β-CH₃ ala), 13.00(β-CH₃ lipid chains); **HRMS (ESI-MS)** calcd. for $\text{C}_{68}\text{H}_{125}\text{N}_7\text{O}_{13}\text{S}$ [$\text{M} + \text{H}$]⁺: calcd. m/z 1280.9134; found: 1280.9126

6.1.6.3. (7R,10S,14R)-7-methyl-3,6,9-trioxo-10-palmitamido-1-(1-(2S,3S,4R,5S,6S)-3,4,5-trihydroxy-6-(hydroxymethyl)tetrahydro-2H-pyran-2-yl)-1H-1,2,3-triazol-4-yl)-12-thia-2,5,8-triazapentadecane-14,15-diyl dipalmitate (6c). Compound **6c** was prepared from compound **5** (100 mg, 0.093 mmol) and 1-azido-β-D-galactose **III** (23 mg, 0.111 mmol) according to the given general procedure in good yield as a white solid. (104 mg, 88%). Melting point: 168–1700C; $^1\text{H NMR}$ (300 MHz, $\text{CDCl}_3 + \text{CD}_3\text{OD}$) δ 8.01 (s, 1H, =CH triazole), 5.49 (d, $J = 9.2$ Hz, 1H, H-1 Gal), 5.24–5.09 (m, 1H, -CH-O ester), 4.52–4.32 (m, 4H, α-CH cys, α-CH-ala and -CH₂-triazole), 4.28 – 3.96 (m, 4H, -CH₂-O ester and -CH₂-gly), 3.92 – 3.62 (m, 6H, H-2, H-3, H-4, H-5, H-6 and H-6), 3.04 – 2.64 (m, 4H, -S-CH₂- and -CH₂-S-), 2.45 – 2.10 (m, 6H, α-CH₂- lipid chains), 1.67–1.52 (m, 6H, β-CH₂-lipid chains), 1.48 – 1.08 (m, 75H, β-CH₃ ala and -CH₂-lipid chains), 0.86 (t, $J = 6.5$ Hz, 9H, -CH₃ lipid chains); $^{13}\text{C NMR}$ (101 MHz, $\text{CDCl}_3 + \text{CD}_3\text{OD}$) δ 174.68(-C=O ester), 173.54(-C=O ester), 173.42(-NHCO-palm), 173.21(-NHCO-peptide), 171.32(-NHCO-peptide), 144.35(=C<, triazole ring), 121.34(=CH, triazole ring), 88.32(C-1 Gal), 77.78(C-5 Gal), 73.46(-CH-O ester), 69.99(C-3 Gal), 69.77(C-4 Gal), 68.55(-CH₂O ester), 63.47(C-2 Gal), 60.84(C-6 Gal), 52.14(α-CH- cys), 49.69(α-CH- ala), 35.57(CH₂-S), 33.87(S-CH₂-), 33.65(α-CH₂- of NHCOpalm), 32.13(α-CH₂- of -COOpalm), 31.46(α-CH₂- of -COOpalm), 29.23, 29.19, 29.10, 28.95, 28.89, 28.68, 25.22, 24.50, 24.44, 22.19(29.23 to 22.19, -CH₂-lipid chain), 16.13(-CH₃ ala), 13.42(-CH₃ lipid chains); **HRMS (ESI-MS)** calcd. for $\text{C}_{68}\text{H}_{125}\text{N}_7\text{O}_{13}\text{S}$ [$\text{M} + \text{H}$]⁺: calcd. m/z 1280.9134; found: 1280.9175

6.1.6.4. (7R,10S,14R)-7-methyl-3,6,9-trioxo-10-palmitamido-1-(1-(2R,3R,4S,5R)-3,4,5,6-tetrahydroxytetrahydro-2H-pyran-2-yl)methyl)-1H-1,2,3-triazol-4-yl)-12-thia-2,5,8-triazapentadecane-14,15-diyl dipalmitate (6d). Compound **6d** can be prepared from compound **5** (100 mg, 0.093 mmol) and 6-azido-D-galactose **IV** (23 mg, 0.111 mmol) according to the above general procedure to afford the compound in good yield as a white solid (114 mg, 96%). Melting Point: 179–1810C; $^1\text{H NMR}$ (300 MHz, $\text{CDCl}_3 + \text{CD}_3\text{OD}$) δ 7.73 (s, 1H, =CH triazole), 5.10 (s, 1H, H-1 galactose), 4.37–4.00 (m, 8H, -CH-O ester, α-CH-cys, α-CH-ala, -CH₂-triazole, 1H-CH₂-O ester, -CH₂-gly), 3.94–3.50 (m, 6H, 1H of -CH₂O ester, H-6, H-6, H-5, H-2, H-3 galactose), 3.46–3.40 (m, C-4 Gal), 2.97–2.55 (m, 4H, -S-CH₂- and -CH₂-S-), 2.35–2.08 (m, 6H, α-CH₂-lipid chains), 1.53 (bs, 6H, β-CH₂-lipid chains), 1.44 – 1.10 (m, 75H, β-CH₃ ala and -CH₂- lipid chains), 0.79 (t, $J = 5.6$ Hz, 9H, -CH₃ lipid chains); $^{13}\text{C NMR}$ (125 MHz, $\text{CDCl}_3 + \text{CD}_3\text{OD}$) δ 175.09(-C=O ester), 175.03 (-C=O ester), 173.62(NH-COpalm), 173.55(-NH-C=O), 171.83 (-NHC=O pept), 169.80(-NHC=O pept), 169.77(-NHC=O pept), 144.42 (=C < triazole ring), 123.68(=C-H triazole ring), 123.42(=CH triazole ring), 96.74(C-1 Gal), 92.35(C-1 Gal), 73.02(-CH-O ester), 71.81 (C-2 Gal), 70.03(C-4 Gal), 69.54(C-4 Gal), 68.80(C-3 Gal), 68.67(C-3 Gal), 68.37(-CH₂-O ester), 63.33(C-5 Gal), 52.41(C-6 Gal), 51.00(α-CH-cys), 50.71(α-CH- cys), 49.93(α-CH- ala), 42.58(-CH₂-gly, -CH₂-triazole ring), 35.55(-CH₂-S-), 34.48(α-CH₂ of -NHCOpalm), 33.99(-S-CH₂-), 33.78(α-CH₂ of -COOpalm), 31.58(α-CH₂ of -COOpalm), 29.35, 29.22, 29.02, 28.79, 25.33, 24.55, 22.32 (29.35 to 22.32, -CH₂- lipid chains) 16.23(β-CH₃ ala), 13.62(-CH₃ of lipid chains); **HRMS (ESI-MS)** calcd. for $\text{C}_{68}\text{H}_{125}\text{N}_7\text{O}_{13}\text{S}$ [$\text{M} + \text{H}$]⁺: calcd. m/z 1280.9134; found: 1280.9172

6.1.6.5. (7R,10S,14R)-1-(1-(2S,3S,4R,5S)-3,4-dihydroxy-5-(hydroxymethyl)tetrahydrofuran-2-yl)-1H-1,2,3-triazol-4-yl)-7-methyl-3,6,9-trioxo-10-palmitamido-12-thia-2,5,8-triazapentadecane-14,15-diyl dipalmitate (6e). Compound **6e** was prepared from compound **5** (100 mg, 0.093 mmol) and 1-azido-ribose **V** (20 mg, 0.111 mmol) according to the general procedure in excellent yield as white solid (114 mg, 98% yield), Melting point: 178–1800C; $^1\text{H NMR}$ (400 MHz, $\text{CDCl}_3 + \text{CD}_3\text{OD}$) δ 7.83

(s, 1H,=CH triazole), 5.73 (s, 1H, H-1 rib), 5.21–5.04 (m, 1H, –CH-O ester), 4.56–4.07 (m, 6H,α-CH-cys, α-CH-ala, –CH₂ of triazole and –CH₂-Oester), 4.06 – 3.73 (m, 6H, –CH₂- gly, H-2,H-3,H-4,H-6, H-6), 2.98–2.62 (m, 4H, -S-CH₂- and –CH₂-S-), 2.40 – 1.96 (m, 6H,α-CH₂-lipid chains), 1.66–1.47 (m, 6H,β-CH₂-lipid chains), 1.46 – 1.05 (m, 75H,β-CH₃ ala and –CH₂- lipid chains), 0.89–0.80 (m, 9H,–CH₃ lipid chains); ¹³C NMR (100 MHz, CDCl₃ + CD₃OD) δ 175.01(–C=O ester), 174.64(–C=O ester), 173.46(–C=O, –NHCO palm), 173.33(–NHCO- pept), 171.67(–NHCO- pept), 85.39(C-1 rib), 70.40(C-4 rib), 69.91(–CH-O ester) 69.37(C-3 rib), 66.24(C-2 rib), 65.06(–CH₂-O ester), 63.19(C-5 rib), 52.42(α-CH-Cys), 52.03(α-CH-ala), 49.72(–CH₂-gly), 49.66(–CH₂-triazole), 35.47(–CH₂-S), 35.25(α-CH₂- -NHCOpalm), 33.76(–S-CH₂), 33.55(α-CH₂-COO ester), 31.38(α-CH₂-COO ester), 29.14, 28.80, 28.58, 25.14, 24.35, 22.10(29.14 to 22.10, –CH₂- lipid chains), 15.96 (β-CH₃ ala), 13.29(–CH₃ lipid chains); HRMS (ESIMS) calcd. for C₆₇H₁₂₃N₇O₁₂S [M + H]⁺: calcd. *m/z* 1250.9028; found: 1250.8999

6.1.6.6. (7R,10S,14R)-1-(1-((S)-2,3-dihydroxypropyl)-1H-1,2,3-triazol-4-yl)-7-methyl-3,6,9-trioxo-10-palmitamido-12-thia-2,5,8-triazapentadecane-14,15-diyl dipalmitate (6f). Compound 6f was prepared from compound 5 (100 mg, 0.093 mmol) and (S)-3-azido-1,2-propane diol VI (13 mg, 0.111 mmol) according to the above general procedure to yield the title compound in good yield (105 mg, 96% yield). White Solid, Melting Point: 169–171 °C; ¹H NMR (400 MHz, CDCl₃ + CD₃OD) δ 7.93 (s, 1H,=CH, triazole ring), 5.33–5.25 (m, 1H, –CH-O ester), 4.73–4.52 (m, 5H,α-CH-cys, α-CH-ala, –CH₂-triazole and 1H of –CH₂-O ester), 4.43 – 4.31 (m, 2H, –CH₂-gly), 4.24–4.16 (m, 1H, –CH₂-Oester), 4.11 (d, *J* = 17.0 Hz, 1H, >N-CH₂-), 3.99 (d, *J* = 16.9 Hz, 1H, >N-CH₂-), 3.79–3.67 (m, 2H, –CH₂-OH), 3.59 (m, 1H, >CH-OH), 3.14 (dd, *J* = 13.9, 6.1 Hz, 1H of -S-CH₂-), 3.01 – 2.81 (m, 3H, –CH₂-S- and 1H of –S-CH₂-), 2.51 (dd, *J* = 14.2, 7.1 Hz, 4H,α-CH₂- 2-ester), 2.46 – 2.31 (m, 2H,α-CH₂- of -NHCOpalm), 1.86–1.68 (m, 6H,β-CH₂-lipid chains), 1.59 (d, *J* = 7.2 Hz, 3H,β-CH₃ ala), 1.44 (bs, 72H, –CH₂- lipid chains), 1.06 (t, *J* = 6.0 Hz, 9H,–CH₃ lipid chains); ¹³C NMR (75 MHz, CDCl₃ + CD₃OD) δ 175.09(–C=Oester), 173.60(–C=O ester), 173.53(–C=O –NHCOpalm, peptide), 171.72(–NHCO- peptide), 144.43(=C < triazole ring), 127.88(=CH, triazole ring) 70.21(–CH-O ester), 70.03(–CH–OH), 63.33(–CH₂-OH), 62.98(–CH₂-Oester), 52.77(–N-CH₂-triazole), 52.42(α-CH₂-Cys), 49.84(α-CH₂-ala), 42.50(–CH₂- gly and –CH₂-triazole), 35.55(–CH₂-S), 34.50(α-CH₂- -NHCOpalm), 33.98(–S-CH₂-), 33.77(α-CH₂- ester), 32.97(α-CH₂-ester), 31.58, 29.34, 29.00, 28.78, 25.32, 24.54, 22.32(31.58 to 22.32, –CH₂- lipid chains), 16.28 (β-CH₃ ala), 13.61(–CH₃, lipid chains); HRMS (ESI-MS) calcd. for C₆₅H₁₂₁N₇O₁₀S [M + H]⁺: calcd. *m/z* 1192.8974; found: 1192.8983

6.1.6.7. (7R,10S,14R)-1-(1-(2-hydroxyethyl)-1H-1,2,3-triazol-4-yl)-7-methyl-3,6,9-trioxo-10-palmitamido-12-thia-2,5,8-triazapentadecane-14,15-diyl dipalmitate (6 g). Titled compound 6 g was prepared from compound 5 (100 mg, 0.093 mmol) and 2-azidoethanol (10 mg, 0.111 mmol) VII according to the general procedure in good yield. (100 mg, 93% yield). White Solid; Melting Point: 166 °C; ¹H NMR (300 MHz, CDCl₃ + CD₃OD) δ 7.78 (s, 1H, triazole ring), 5.18–5.07 (m, 1H, –CH-Oester), 4.48 – 4.33 (m, 4H,α-CH-cys, α-CH-ala, –CH₂-triazole), 4.27 – 4.08 (m, 6H, –CH₂-gly, –CH₂-Oester & –CH₂-OH), 3.91 (t, *J* = 5.1 Hz, 2H, -N-CH₂-), 2.93 (dd, *J* = 13.5, 6.3 Hz, 2H, -S-CH₂-), 2.76 (dd, *J* = 19.0, 7.1 Hz, 2H-CH₂-S-), 2.31 (dd, *J* = 11.4, 7.4 Hz, 4H,α-CH₂- of ester), 2.25 – 2.10 (m, 2H,α-CH₂- of -NHCOpalm), 1.66–1.48 (m, 6H, β-CH₂-lipid chains), 1.39 (d, *J* = 7.2 Hz, 3H,β-CH₃ ala), 1.24 (bs, 75H, –CH₂-lipid chains), 0.85 (t, *J* = 6.5 Hz, 9H,3-CH₃ lipid chains). ¹³C NMR (75 MHz, CDCl₃ + CD₃OD) δ 174.87(–C=O ester), 173.35(–C=O ester and palm amide), 173.15(–C=O pept), 171.52(–C=O pept), 169.66(–C=O pept), 143.95(=C < triazole ring), 123.17(=CH, triazole ring) 69.86(–CH- ester), 63.09(–CH₂- ester), 59.88(–CH₂-OH), 52.38(–N-CH₂- triazole), 52.16(α-CH- cys), 49.60(α-CH- ala), 42.08(–CH₂- gly, triazole) 35.13(–CH₂-S-), 34.11(α-CH₂- -NHCOpalm), 33.62(–S-CH₂-),

33.41(α-CH₂- of ester), 32.78(α-CH₂- ester), 31.41, 31.27, 29.02, 28.69, 28.45, 25.05, 24.26, 21.98(31.41 to 21.98, –CH₂-lipid chains), 15.78 (β-CH₃ ala), 13.08(–CH₃ lipid chains); (ESIMS) calcd. for C₆₄H₁₁₉N₇O₉S [M + Na]⁺: calcd. *m/z* 1184.8690; found: 1184.8698

Declaration of Competing Interest

The authors declare that they have no known competing financial interests or personal relationships that could have appeared to influence the work reported in this paper.

Acknowledgement

TM and SS thank CSIR and DST for the award of fellowships. Authors thank DST, New Delhi for the financial support through Grant-in-aid project GAP0774. CSIR-IICT Manuscript No: IICT/Pubs./2019/365

Appendix A. Supplementary material

Supplementary data to this article can be found online at <https://doi.org/10.1016/j.bioorg.2021.104838>.

References

- [1] D.T. O'Hagan, E. De Gregorio, The path to a successful vaccine adjuvant 'the long and winding road', *Drug Discov Today*. 14 (11–12) (2009) 541–551, <https://doi.org/10.1016/j.drudis.2009.02.009>.
- [2] Marie L. Hecht, Pierre Stallforth, Daniel V. Silva, Alexander Adibekian, Peter H. Seeberger, Recent advances in carbohydrate-based vaccines, *Curr. Opin. Chem. Biol.* 13 (3) (2009) 354–359. ISSN 1367-5931.
- [3] D.R. Bundle, A carbohydrate vaccine exceeds the sum of its parts, *Nat. Chem. Biol.* 3 (10) (2007) 605–606, <https://doi.org/10.1038/nchembio1007-605>.
- [4] A.O. Aliprantis, R.B. Yang, M.R. Mark, et al., Cell activation and apoptosis by bacterial lipoproteins through toll-like receptor-2, *Science* 285 (5428) (1999) 736–739, <https://doi.org/10.1126/science.285.5428.736>.
- [5] K. Takeda, T. Kaisho, S. Akira, Toll-like receptors, *Annu. Rev. Immunol.* 21 (2003) 335–376, <https://doi.org/10.1146/annurev.immunol.21.120601.141126>.
- [6] M.V. Spanedda, B. Heurtault, S. Weidner, et al., Novel powerful water-soluble lipid immunoadjuvants inducing mouse dendritic cell maturation and B cell proliferation using TLR2 pathway, *Bioorg. Med. Chem. Lett.* 20 (6) (2010) 1869–1872, <https://doi.org/10.1016/j.bmc.2010.01.146>.
- [7] I. Fernandes, B. Frisch, S. Muller, F. Schuber, Synthetic lipopeptides incorporated in liposomes: in vitro stimulation of the proliferation of murine splenocytes and in vivo induction of an immune response against a peptide antigen, *Mol. Immunol.* 34 (8–9) (1997) 569–576, [https://doi.org/10.1016/S0161-5890\(97\)00090-4](https://doi.org/10.1016/S0161-5890(97)00090-4).
- [8] A. Roth, S. Espuelas, C. Thumann, B. Frisch, F. Schuber, Synthesis of thiol-reactive lipopeptide adjuvants. incorporation into liposomes and study of their mitogenic effect on mouse splenocytes, *Bioconjugate Chem.* 15 (2004) 541–553.
- [9] F. Reichel, A.M. Roelofsen, H.P.M. Geurts, S.J. van der Gaast, M.C. Feiters, G.-J. Boons, Synthesis and supramolecular characterization of a novel class of glycopyranosyl-containing amphiphiles, *J. Org. Chem.* 65 (11) (2000) 3357–3366, <https://doi.org/10.1021/jo991685s>.
- [10] Sohne Voss, Artur J. Ulmer, Gunther Jung, Karl-Heinz Wiesmuller, Roland Brock, The activity of lipopeptide TLR2 agonists critically depends on the presence of solubilizers, *Eur. J. Immunol.* 37 (2007) 3489–3498.
- [11] F.M. Veronese, G. Pasut, PEGylation, successful approach to drug delivery, *Drug Discov. Today*. 10 (21) (2005) 1451–1458, [https://doi.org/10.1016/S1359-6446\(05\)03575-0](https://doi.org/10.1016/S1359-6446(05)03575-0).
- [12] N. Nalla, P. Pallavi, B.S. Reddy, S. Miryala, V. Naveen Kumar, M. Mahboob, M. S. Halmuthur, Design, synthesis and immunological evaluation of 1,2,3-triazole-tethered carbohydrate-Pam3Cys conjugates as TLR2 agonists, *Bioorg. Med. Chem.* 23 (17) (2015) 5846–5855, <https://doi.org/10.1016/j.bmc.2015.06.070>.
- [13] S. Velázquez, R. Alvarez, C. Pérez, F. Gago, E. De Clercq, J. Balzarini, M.-J. Camarasa, Regiospecific synthesis and anti-human immunodeficiency virus activity of novel 5-substituted N-alkylcarbamoyl and N, N-dialkyl carbamoyl 1,2,3-triazole-TSAO analogues, *Antiviral Chem. Chemother.* 9 (1998) 481–489.
- [14] X.M. Chen, Z.J. Li, Z.X. Ren, Z.T. Huang, Synthesis of glucosylated 1,2,3-triazole derivatives, *Carbohydr Res.* 315 (3–4) (1999) 262–267, [https://doi.org/10.1016/S0008-6215\(99\)00020-8](https://doi.org/10.1016/S0008-6215(99)00020-8).
- [15] P.K. Kadaba, 1, 2, 3-Triazolines and triazoles. A new class of anticonvulsants. *Drug design and structure-activity relationships, J. Med. Chem.* 31 (1) (1988) 196–203.
- [16] Derek R. Buckle, Caroline J.M. Rockell, Harry Smith, Barbara A. Spicer, Studies on 1,2,3-triazoles; (Piperazinylalkoxy)-[1]benzopyrano[2,3-d]-1,2,3-triazol-9(1H)-ones with combined H1-antihistamine and mast cell stabilizing properties, *J. Med. Chem.* 29 (11) (1986) 2262–2267, <https://doi.org/10.1021/jm00161a022>.
- [17] C.B. Vicentini, V. Brandolini, M. Guarneri, P. Giori, Pyrazolo[3,4-d][1,2,3]triazole-1-carboxamides and 5-alkylaminopyrazolo[3,4-d]oxazoles: synthesis and evaluation of the in vitro antifungal activity, *Farmaco* 47 (7–8) (1992) 1021–1034.

- [18] T. Lee, M. Cho, S.Y. Ko, et al., Synthesis and evaluation of 1,2,3-triazole containing analogues of the immunostimulant alpha-GalCer, *J. Med. Chem.* 50 (3) (2007) 585–589, <https://doi.org/10.1021/jm061243q>.
- [19] Yogesh Kumar Verma, Bonam Srinivasa Reddy, Mithun S. Pawar, Debabrata Bhunia, Halmuthur M. Sampath, Kumar, Design, synthesis, and immunological evaluation of benzyloxyalkyl-substituted 1,2,3-triazolyl α -GalCer analogues, *ACS Med. Chem. Lett.* 7 (2) (2016) 172–176, <https://doi.org/10.1021/acsmchemlett.5b00340>.
- [20] Mohamed R. Aouad, Synthesis and antimicrobial screening of novel thioglycosides analogs carrying 1,2,3-triazole and 1,3,4-oxadiazole moieties, *Nucl., Nucl. Acids* 35 (1) (2016) 1–15.
- [21] Nadjet Rezki, Mariem Mohammed Mayaba, Fawzia Faleh Al-blewi, El Sayed Helmi El Ashry, Mohamed Reda Aouad, Click 1,4-regioselective synthesis, characterization, and antimicrobial screening of novel 1,2,3-triazoles tethering fluorinated 1,2,4-triazole and lipophilic side chain, *Res. Chem. Intermed.* 43 (2017) 995–1011.
- [22] Mohamed Reda Aouad, Click synthesis and antimicrobial screening of novel isatin-1,2,3-triazoles with piperidine, morpholine or piperazine moieties, *Org. Prep. Proced. Int.* 49 (2017) 216–227.
- [23] Mohamed Reda Aouad, Mariem Mohammed Mayaba, Arshi Naqvi, Sanaa K. Bardaweel, Fawzia Faleh Al-blewi, Mouslim Messali, Nadjet Rezki, Design, synthesis, in-silico and in-vitro antimicrobial screenings of novel 1,2,4-triazoles carrying 1,2,3-triazole scaffold with lipophilic side chain tether, *Chem. Cent. J.* 11 (2017) 117–129.
- [24] Fawzia Faleh Al-blewi, M.A. Almeahmadi, Mohamed Reda Aouad, Sanaa K. Bardaweel, Pramod K. Sahu, Mouslim Messali, Nadjet Rezki, El Sayed H. El Ashry, Design, synthesis, ADME prediction and pharmacological evaluation of novel benzimidazole-1,2,3-triazole-sulfonamide hybrids as antimicrobial and antiproliferative agents, *Chem. Cent. J.* 12 (2018) 110–123.
- [25] Mohamed R. Aouad, Moataz A. Soliman, Muath O. Alharbi, Sanaa K. Bardaweel, Pramod K. Sahu, Adeeb A. Ali, Mouslim Messali, Nadjet Rezki, Yaseen A. Al-Soud, Design, synthesis and anticancer screening of novel benzothiazole-piperazine-1,2,3-triazole hybrids, *Molecules* 23 (2018) 2788–2801.
- [26] Mohamed Reda Aouad, Meshal A. Almeahmadi, Nadjet Rezki, Fawzia Faleh Al-blewi, Mouslim Messali, Imran Ali, Design, click synthesis, anticancer screening and docking studies of novel benzothiazole-1,2,3-triazoles appended with some bioactive benzofused heterocycles, *J. Mol. Struct.* 1188 (2019) 153–164.
- [27] Nadjet Rezki, Meshal A. Almeahmadi, Saleh Ihmaid, Ahmed M. Shehata, Abdelsattar M. Omare, Hany E.A. Ahmed, Mohamed Reda Aouad, Novel scaffold hopping of potent benzothiazole and isatin analogues linked to 1,2,3-triazole fragment that mimic quinoxaline epidermal growth factor receptor inhibitors: synthesis, antitumor and mechanistic analyses, *Bioorg. Chem.* 103 (2020) 104133–104147.
- [28] Meshal A. Almeahmadi, Ateyatallah Aljuhani, Shaya Yahya Alraqa, Imran Ali, Nadjet Rezki, Mohamed Reda Aouad, Mohamed Hagar, Design, synthesis, DNA binding, modeling, anticancer studies and DFT calculations of Schiff bases tethering benzothiazole-1,2,3-triazole conjugate, *J. Mol. Struct.* 1225 (2021) 129148–129162.
- [29] Shaya Yahya Alraqa, Khalid Alharbi, Ateyatallah Aljuhani, Nadjet Rezki, Mohamed Reda Aouad, Imran Ali, Design, click conventional and microwave syntheses, DNA binding, docking and anticancer studies of benzotriazole-1,2,3-triazole molecular hybrids with different pharmacophores, *J. Mol. Struct.* 1225 (2021), 129192.
- [30] Biswajit Kumar Singh, Amit Kumar Yadav, Brijesh Kumar, A. Gaikwad, Sudhir Kumar Sinha, Vinita Chaturvedi, Rama Pati Tripathi, Preparation and reactions of sugar azides with alkynes: synthesis of sugar triazoles as antitubercular agents, *Carbohydr. Res.* 343 (7) (2008) 1153–1162, <https://doi.org/10.1016/j.carres.2008.02.013>.
- [31] Abdul Rouf, Mushtaq A. Aga, Brijesh Kumar, Subhash Chandra Taneja, A facile approach to chiral 1,4-benzodioxane toward the syntheses of doxazosin, prosympal, piperoxan, and dibozane, *Tetrahedron Lett.* 54 (48) (2013) 6420–6422, <https://doi.org/10.1016/j.tetlet.2013.09.040>.
- [32] Nalla Naresh, Preethi Pallavi, Bonam Srinivasa Sreekanth Miryala, V. Naveen Kumar, Mohammad Mahboob, Halmuthur M. Sampath Kumar, Design, synthesis and immunological evaluation of 1,2,3-triazole-tethered carbohydrate–Pam3Cys conjugates as TLR2 agonists, *Bioorg. Med. Chem.* 23 (2015) 5846–5855.
- [33] Caterina Spezzacatena, Tiziana Perri, Valeria Guantieri, Lawrence B. Sandberg, Thomas F. Mitts, Antonio M. Tamburro, Classical synthesis of and structural studies on a biologically active heptapeptide and a nonapeptide of bovine elastin, *Eur. J. Org. Chem.* 1 (2002) 95–103.
- [34] Alejandro J. Cagnoni, Oscar Varela, Sebastien G. Gouin, Jose Kovensky, Maria Laura Uhrig, Synthesis of multivalent glycoclusters from 1-thio- β -D-galactose and their inhibitory activity against the β -galactosidase from *E. coli*, *J. Org. Chem.* 76 (9) (2011) 3064–3077.
- [35] Concepción Badia, Florence Souard, Cristina Vicent, Sugar-oligoamides: synthesis of DNA minor groove binders, *J. Org. Chem.* 77 (23) (2012) 10870–10881, <https://doi.org/10.1021/jo302238u>.
- [36] Cindy J. Carroux, Janina Moeker, Josephine Motte, Marie Lopez, Laurent F. Bornaghi, Kasiram Katneni, Eileen Ryan, Julia Morizzi, David M. Shackleford, Susan A. Charman, Sally-Ann Poulsen, Synthesis of acylated glycoconjugates as templates to investigate in vitro biopharmaceutical properties, *Bioorg. Med. Chem. Lett.* 23 (2) (2013) 455–459, <https://doi.org/10.1016/j.bmcl.2012.11.056>.
- [37] J. Yang, X. Fu, Q. Jia, J. Shen, J.B. Biggins, J. Jiang, J. Zhao, J.J. Schmidt, P. G. Wang, J.S. Thorson, Studies on the substrate specificity of *Escherichia coli* galactokinase, *Org. Lett.* 5 (13) (2003) 2223–2226, <https://doi.org/10.1021/ol034642d>.
- [38] Peter Ten Holte, Bart C.J. Van Esseveldt, Lambertus Thijs, Binne Zwanenburg, Synthesis of oxazolidinones by a Solid phase/Activation Cycloelimination(SP/ACE) methodology, *Eur. J. Org. Chem.* 15 (2001) 2965–2969.
- [39] Jin-Cheng Wu, De-Xian Wang, Zhi-Tang Huang, Mei-Xiang Wang, Synthesis of diverse N, O-bridged calix[1]arene[4]pyridine-C60 dyads and triads and formation of intramolecular self-inclusion complexes, *J. Org. Chem.* 75 (24) (2010) 8604–8614, <https://doi.org/10.1021/jo1019267>.
- [40] S.K. Gandhapudi, P.M. Chilton, T.C. Mitchell, TRIF is required for TLR4 mediated adjuvant effects on T cell clonal expansion, *Public Libr. Sci.* 8 (2) (2013), e56855.
- [41] Martina Barrenschee, Dennis Lex, Stefan Uhlig, Effects of the TLR2 agonists MALP-2 and Pam3Cys in isolated mouse lungs, *J. Mol. Biol.* 5 (11) (2010) e13889.